Fall 2016

Longitudinal Tidal Dispersion Coefficient Estimation and Total Suspended Solids Transport Characterization in the James River

Beatriz Eugenia Patino
Old Dominion University, beatriz_epr@hotmail.com

LONGITUDINAL TIDAL DISPERSION COEFFICIENT ESTIMATION AND TOTAL SUSPENDED SOLIDS TRANSPORT CHARACTERIZATION IN THE JAMES RIVER

by

Beatriz E. Patino
B.S. November 2002, Universidad del Valle, Colombia

A Thesis Submitted to the Faculty of
Old Dominion University in Partial Fulfillment of the
Requirements for the Degree of

MASTER OF SCIENCE

ENVIRONMENTAL ENGINEERING

December 2016

Approved by:

Jaewan Yoon (Director)

Xixi Wang (Member)

Ben Stuart (Member)

ABSTRACT

LONGITUDINAL TIDAL DISPERSION COEFFICIENT ESTIMATION AND TOTAL SUSPENDED SOLIDS CHARACTERIZATION IN THE JAMES RIVER

Beatriz E. Patino
Old Dominion University, 2016
Director: Dr. Jaewan Yoon

The longitudinal dispersion coefficient is a parameter used to evaluate the effect of cross-sectional variations on substance mixing mechanisms in estuaries influenced by tide, wind and internal density variations. Considering a two dimensional approach, this study aims at evaluating a tidal area of the lower James River at approximately 19 miles upstream from the mouth at the Chesapeake Bay, in the City of Newport News, and applies an experimental procedure based on in-situ salinity concentrations to estimate the dispersion coefficient in the area where receives a discharge from the HRSD James River Wastewater Treatment Plant, and further characterizes Total Suspended Solids (TSS) mixing and transport mechanisms in the surrounding area. In-situ data collection was carried out twice a day during two consecutive days (July 21st and July 22nd, 2016) to measure salinity, turbidity, temperature and velocity. Subsequently, Control Volume (CV) approach method with Steady State Response Matrix (SSRM) was applied to characterize the transport mechanism of Total Suspended Solids among eight segments in the study area, with two of them acting as boundary conditions. Statistical General Linear Model (GLM) method was used to develop in-situ correlationship between Turbidity and Total Suspended Solids from historical HRSD James River plant data series during the years 2001 through 2015. Then measured Turbidity values were used to estimate corresponding Total Suspended Solids concentrations used in the study. The results obtained during this research suggest that in the study area of the James river, dispersive mechanisms of Flood cycles influence the transport of TSS towards the upstream, reducing the effect of advective movement from the Warwick River towards the lower reach of the James.

I dedicate this accomplishment to my dad, who departed without the opportunity of seeing me achieve this goal, who motivated me to follow my career in Sanitary Engineering and was always interested in my area of study, providing me with his knowledge and expertise in Environmental Law, guiding me through my professional career. To him, who was always proud of his children, who always believed in us and who departed with the satisfaction of having accomplished his mission in life.

ACKNOWLEDGMENTS

I would like to thank my committee members for providing their time, knowledge and experience in reviewing this document and giving the necessary guidance and criticisms to successfully complete this research.

I would like to give special thanks to my advisor Dr. Jaewan Yoon, who since the first semester willingly accepted to be my advisor without doubt and without even know me enough to make his decision. His support, understanding and encouragement throughout all these semesters motivated me to initiate this research and his guidance facilitate the selection of the courses needed to route my masters in the right direction for the aspirations on my professional career.

I would also want to thank the professors at Old Dominion University from which I had the opportunity to learn and interact over the past two years, in special Dr. Mudje Erten-Unal and Dr. Xixi Wang who were always willing to help and to share their knowledge openly to all of their students. Having the opportunity of taking their courses was a personal and professional growing and learning experience.

Finally, I want to thank my parents, German and Beatriz, for teaching us how to persevere in life and always do our best, to my siblings, Angela and German for their continue support and for believing in me. Specially, I want to thank my children, my unborn child and my lovely daughter, Ana who has been the greatest motivation for doing all the things I have done in life since I had her. Finally, infinite thanks to my fiancée Gianluigi; without his love, understanding, patience and support I could not have achieved this goal in the way I did.

TABLE OF CONTENTS

Page

LIST OF TABLES

Table Page

LIST OF FIGURES

Figure Page

CHAPTER 1.

LONGITUDINAL DISPERSION COEFFICIENT ESTIMATION IN ESTUARIES

1.1. Introduction

Understanding substance mixing and transport phenomena is fundamental and essential processes to correctly predict the fate of any pollutant in the aquatic environment, and subsequently evaluate the attainability of desired water quality standards *in loco*. Resultant reactivity and physical transport per substance vary depending on the substance characteristic and corresponding mechanisms and processes of mass transport -- Advection, Diffusion and Dispersion, receiving body of water, and other environmental conditions.

When a pollutant enters surface water, physical processes such as advection and dispersion, and spatial velocity distribution dominates the initial mixing and spatiotemporal spread of the pollutant in the adjacent areas. In rivers and streams where advection dominates, dispersive transport due to mixing is generally small compared with advective transport (Martin, 1999). Estuaries, on the other hand, are coastal bodies of water with free connection to the open sea that have complex temporal transport and circulation processes controlled by tides and freshwater influx. So that bidirectional flow and dispersive motion incur dynamic and complex progressions in flow, velocity and depth as well as result mixing and transport mechanisms.

Dispersion and mixing processes in estuaries are greatly influenced by intrinsic salinity distribution. For instance, in highly salinity-stratified polyhaline estuaries, despite weak mass exchange among the interfacial region, effective vertical mixing within each layer is more pronounced. The existence of stratification as well as complex tidal fluctuations modifies the effects of vertical mixing and friction and therefore dispersion of substances introduced in low-level outfalls has evidenced markedly differences from dispersion of those introduced into the freshwater flow (Martin *et al.*, 1999). Thus salinity gradients can be used effectively to estimate segmental dispersion coefficients in estuaries. The longitudinal dispersion coefficient is a complex parameter applied to describe the turbulent diffusivity driven by the velocity distribution in an estuarine segment, and its numerical value varies significantly depending on the influence from freshwater discharge, tidal variations, bed friction, channel topography and density gradients (Shana *et al.*, 2011).

In terms of transport and fate modeling approach, dispersion is typically applied in one or two dimensional models or when averaging transport over a recurring event such a tidal cycle, where non-uniformities in velocities, temperatures or concentrations prevail.

On the other hand, one dimensional models are applicable when topography and bathymetry of the estuary result in a long, narrow and sufficiently unstratified condition, then flow velocity, salinity and concentration of any dissolved substance are assumed to be dependent only on the relative distance from the mouth of the estuary. Under one dimensional approximation, all mixing mechanisms aggregate into one single longitudinal dispersion coefficient that is typically determined by using natural tracers such as salinity gradient (Fischer, 1979).

1.2. Factors affecting Dispersion, Mixing and Transport in Estuaries

To understand the mixing phenomena in estuaries, it is necessary to first evaluate spatiotemporal variability in physical processes in the body of water. According with Fischer (1979) and Martin *et al.* (1999), the most important factors influencing dispersion, mixing and transport of substances in estuaries are tides, Coriolis force, freshwater inflow and meteorological effects.

Tides:

Ocean tides are produced by interaction of the gravitational fields of the earth, moon and sun. The effect of tides causes (1) time-variable mixing through frictional interaction with the bottom and overlying freshwater flows, and (2) spatially asymmetric flow patterns during ebb and flood through interaction with the bottom topography. Tides are expressed in terms of amplitude and tidal current (over ebb and flood velocity fields). The tide amplitude refers to the variation of water level about a datum level, which is produced by the effect of moon and solar gravitational fields, commonly known as spring and neap tidal cycles.

Tidal waves can be treated as long-period within a linear system composed of a number of tidal constituents representing the periodic change in the relative positions of the earth, moon and sun (Fig. 1.1.).

$$\zeta(t) = \zeta_0 + \sum_{i=1}^{N} f_i h_i \cos(\omega_i t + \alpha_i) \qquad \text{Eq. (1.1)}$$

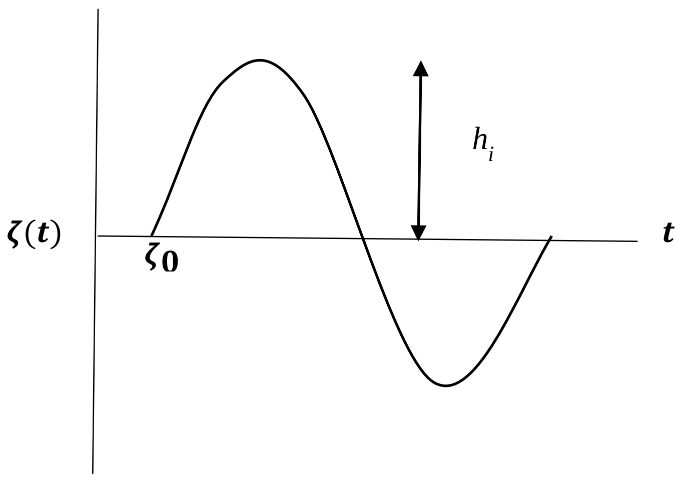

Fig. 1.1. Tidal wave configuration

where $\zeta(t)$ is the total variation of the water surface elevation at time t and N is the number of tidal constituents necessary to describe the time-varying water surface elevations at a specific location. ζ_0 is the mean height above some datum, f_i is a dimensionless factor for reducing the mean amplitude to the year of prediction, h_i is the tidal amplitude, ω_i is the angular speed of the tidal constituent, α_i the phase shift and t is the time. Tidal current characteristic in estuaries varies significantly with horizontal water movements associated with the rising and falling tides. Each time the water changes directions there is a period of no net current, known as the slack water. (Martin *et al.*, 1999).

Another variation in tidal circulation and mixing patterns would occur when a particle become "trapped" during flood tide and remain in a specific location until ebb tide move it out of the embayment. This process is known as "tidal trapping" and it is associated to changes in bathymetry that creates velocity variations and turbulence.

The Coriolis force:

The Coriolis force affects wide and open estuaries resulting in all objects in motion on the earth's surface to be deflected to the right in the northern hemisphere, or left in the southern

(Martin *et al.,.* 1999). In the northern hemisphere, less-dense water in wide estuaries affected by this force, moves to the right, while in the southern hemisphere, moves to the left. The relative importance of the Coriolis force can be estimated from the dimensionless Rossby number (R_0), which is the ratio of the period of rotation to the time of advection (Fischer *et al.*,. 1979), given by:

$$R_0 = \frac{U}{L_s f} \qquad \text{Eq. (1.2)}$$

where

U = Horizontal velocity of the current

L_s = Characteristic length scale for the estuary such as its width.

f = Coriolis parameter

When Rossby numbers (R_0 <0.1) are in a low range, Coriolis effect is considered as an important factor for dispersion, mixing and transport of substances in estuaries.

Freshwater inflow:

Magnitude of freshwater flowing into an estuary has a significant impact on mixing characteristic. In some estuaries, the volume of freshwater is sufficient to maintain a density differential over large distances before being completely mixed into seawater. Increased freshwater inflow can change the character of an estuary from well-mixed to partially mixed or stratified in a wedge-shaped layer formation. Decreased inflow can have the opposite effect with a concomitant increased upstream intrusion of seawater. Freshwater inflows can also affect the duration of the flood and slack currents. As a result, the ebb current often lasts longer than the flood current (Martin *et al.*, 1999).

Meteorological effects:

Meteorological effects include wind forcing and atmospheric pressure forcing. Wind effects include generation of circulation patterns by seasonal weather, modification of circulation patterns by localized weather and generation of waves and storm surges (Martin *et al.*, 1999).

The effects of winds vary with the wind speed, direction, duration and size and shape of the estuary. Winds can result in wave action, promoting vertical mixing while surface currents can form due to sustained winds.

In stratified estuaries, the effects of winds may be restricted to surface layers. In estuaries with relatively small freshwater inflows and with a small tidal range, wind is the dominant force in driving the overall circulation and in generating turbulent mixing (Martin *et al.*, 1999).

1.3. Estuaries Dispersion Coefficient Estimation

Fischer (1979) indicated that mixing in estuaries results from a combination of small scale turbulent diffusion and larger scale variation of advective mean velocities. The main role of turbulent diffusion is to transfer mass between stream lines while longitudinal dispersion manifests when flows along with different stream lines are going at different speeds.

Dispersion is considered as a turbulent eddy gradient process, and its magnitude will depend on the shear in the horizontal velocity, combined with the vertical turbulent diffusion. The dispersion increases as the rate of diffusion decreases (Dyer, 1997). Dispersion coefficient, E, is defined as the ratio of the non-advective transport rate of salt (or other substances) through a unit cross-sectional area to the salinity gradient along the main axis of the estuary (Shana *et al.,* 2011). Thus dispersion coefficient is an essential component to describe and characterize complex substance mixing and transport phenomena occurring in the estuarine body of water.

To express the diffusive property of the velocity distribution in the water, a parameter, longitudinal dispersion coefficient, E_x, is used to express the effect of cross sectional variations and mixing mechanisms in estuaries contributed by tide, wind and internal density variations.

Larger dispersion coefficient values are expected in the salinity intrusion region of the estuaries compared to the ones found in the freshwater tidal portion. The dispersion coefficient in the fresh water portion accounts for the longitudinal mixing due to turbulent diffusion and shear induced velocity distribution in the transverse and vertical directions. In the saline portion, the velocity distribution is less uniform and the dispersion coefficient is closely related to gravitational circulation that depends on the salinity distribution. (Wilber, 1986)

According with Schnoor (1996), there are no simple formulas to estimate the longitudinal dispersion coefficient in an estuary. It can be experimentally obtained from:

- Spatiotemporal salinity data over tidal cycles
- Spatial distribution of dye (tracer) experiments
- Temporal distribution of dye (tracer) experiments

Estimation of Dispersion coefficient from salinity data in an estuary:

As salinity decreases from the ocean to the upstream brackish portion of the salinity intrusion, it is considered as the “nature’s own tracer” of the longitudinal dispersion in an estuary (Schnoor, 1996). A mass balance differential equation for salinity, a conservative substance, at steady state is expressed by:

$$E\frac{d^2S}{dx^2} - u\frac{dS}{dx} = 0 \qquad \text{Eq. (1.3)}$$

Applying boundary conditions

B.C. 1 : $S = S_0$ at $x = 0$

B.C. 2 : $S = 0$ at $x = -\infty$

then the general solution yields to

$$S = S_0 e^{ux/E} \quad for\ x \le 0$$

$$S = S_0 \quad for\ x > 0 \qquad \text{Eq. (1.4)}$$

where

S = Salinity concentration, ML^{-3}

S_0 = Initial concentration at $x = 0$, ML^{-3}

u = Net (tidal-averaged) velocity due to freshwater flow, LT^{-1}

x = Distance from the mouth to upstream river (negative values), -L

E = Dispersion coefficient, L^2T^{-1}

The final equation is derived after taking natural log, and then it can be used to obtain the average longitudinal dispersion coefficient, E from the inverse of the slope.

$$ln\frac{S}{S_0} = \frac{U}{E}x \qquad \text{Eq. (1.5)}$$

Estimation of Dispersion coefficient from Dye (tracer) data in an estuary:

Dyes such as fluorescent Rhodamine WT are often used to determine the mixing and transport characteristics of a substance effluxed into a natural water body. For large rivers and estuaries, the tracer can be assumed to be well mixed with depth and across the channel (lateral or transverse direction). (Schnoor, 1996).

Dye studies are generally performed during high water slack tide and low water slack tide with the purpose of obtaining accurate measurements of non-tidal velocity. Either an impulse discharge or a continuous input of dye can be administered at an upstream location. Measured mass concentration distribution at downstream from the injection point can be used to determine parameters such as velocity and dispersion coefficient (Chapra, 2008).

General mass balance partial differential equation that describes an impulse discharge to a 1-D estuary is given by:

$$\frac{\partial C}{\partial t} = \frac{1}{A}\frac{\partial}{\partial x}\left(EA\frac{\partial C}{\partial x}\right) - \frac{1}{A}\frac{\partial}{\partial x}(QC) - kC \qquad \text{Eq. (1.6)}$$

where *C* is the concentration of the dye tracer (ML^{-3}) and *k* is the first-order degradation rate constant (T^{-1}) if the dye contains a non-conservative substance.

Under a steady flow conditions (tidal-averaged) and relatively constant cross sectional area, equation Eq. (1.6) can be simplified and its general solution for an 1-D estuary can be derive by the integration as shown in Eq. (1.7). Eq. (1.7) is then further transformed into a linearized form given in Eq. (1.8) to estimate the dispersion coefficient, E.

$$C = \frac{M}{2A\sqrt{\pi Et}}exp\left[\frac{-(x-ut)^2}{4Et} - kt\right] \qquad \text{Eq. (1.7)}$$

$$lnC = \frac{-\phi^2}{4Et} + ln\left(\frac{M}{2A\sqrt{\pi Et}}\right) - kt \qquad \text{Eq. (1.8)}$$

where

C = Concentration of dye, ML^{-3}

Φ = (x-ut) = Distance of the dye measurement from the peak concentration, L

M = Mass of dye injected, M

A = Average cross-sectional area of the estuary, L^2

E = Longitudinal dispersion coefficient, L^2T^{-1}

t = Time since release of the dye

x = longitudinal distance with x = 0 being the location where the dye was released and downstream distance is positive, L

u = Net non-tidal velocity, LT^{-1}

k = Sum of the first-order reaction rate coefficients for disappearance of the dye, T^{-1}

Thus, spatial distribution of dye mass concentration is expressed in Eq. (1.8), and a plot of lnC versus ϕ^2 will yield a straight line with slope, which is $-1/(4Et)$.

1.4. Problem Conceptualization

Water quality modeling in estuaries requires analysis on factors that influence hydrodynamic and hydromorphologic processes of the estuarine body expressed with a combination of advective and dispersive transport phenomena. Among these factors, tidal fluctuations is one of the most influential in forms of freshwater discharge and salt water intrusion fluxes that will dictates a particular dominance of either advective or dispersive transport in the estuarine body. A fundamental parameter describing such dominance in transports is the dispersion coefficient, E. Dispersion coefficient is highly site-specific, and is essential to accurately represent the effect of cross-sectional variations and mixing mechanisms in estuaries caused by tide, wind and internal density variations.

Estimation of dispersion coefficient in estuaries is a complex process compared to that of unidirectional stream and riverine environments, and in most cases it includes a release of dye at a controlled source location followed by continuous monitoring at selected number of stations over multiple tidal cycles. Alternatively, estuarine dispersion coefficient can be estimated by the application of the salt balance equation that uses the natural salt gradient presented in different segments of the estuary along with the averaged velocity over multiple tidal cycles.

There are few of previous water quality studies that had estimated dispersion coefficients for selected tributary rivers into the Chesapeake Bay such as the study carried out in the James River at the Nansemond River mouth by Dr. Albert Kuo of the Virginia Institute of Marine Science (VIMS) in 1974 in which a method for predicting the concentration distribution of a sewage effluent in the James River from a location where a sewage outfall of the Nansemond Sewage Treatment Plant was proposed to be built. Another study was conducted in the Rappahannock River by Anne Catherine Wilber in 1986, whose purpose was to predict the dispersion coefficient considering the effect of vertical shear and transverse shear of the tidal flow in the freshwater portion of the estuary and the effects of gravitational circulation in the saline portion of the estuary. Yet the overwhelming majority of these studies were based upon the segmentation of the river over an extensive longitude (~ 20 Km) that estimated dispersion coefficients were in a very low-resolution and may not facilitate a necessary spatial accuracy required for predicting complex mixing and transport phenomena of substance in a finer scale or in a smaller area

In this study, in-situ samplings of the natural salt gradient at a tidal section of the James River were collected to estimate dispersion coefficients, then Total Suspended Solids mixing and transport phenomena in a tidal area of influence receiving the HRSD James River Treatment Plant discharge were characterized by using a Control Volume (CV) Finite Segment Method (FSM).

1.5. Objectives

Objective of this study is to estimate high-resolutioned, in-situ dispersion coefficients in the area of the James River in Newport News where receives an effluent discharge from the HRSD James River Wastewater Treatment Plant, and to characterize subsequent advective and dispersive transports of Total Suspended Solids in its estuarine body of water. The main objectives are:

- To use spatiotemporal salinity concentration measurements over tidal cycles to estimate site-specific longitudinal and lateral tidal dispersion coefficients in a small area of the lower James River influenced by the Warwick River inflow and the James River Wastewater Treatment Plant

- To develop a site-specific General Linear Model (GLM) by utilizing historical TSS/Turbidity data pair series obtained from the James River Treatment Plant, and to estimate TSS concentrations from Turbidity measurement collected in situ in this study
- To apply the Finite Segment Method (FSM) and the Steady State Response Matrix (SSRM) to characterize Total Suspended Solids mixing and transport mechanisms in the study area with Control Volume (CV) approach and compare the estimated results under per tidal cycle and per tidally averaged cycles.

CHAPTER 2.

LITERATURE REVIEW

As previously discussed, dispersion is the primary factor controlling speed, magnitude and direction of transport of substances introduced in estuaries, and magnitude of dispersion is highly influenced by the longitudinal cross-sectional variation of velocities in the water. Subsequently, corresponding dispersion coefficient is a very site-specific parameter, and is required to be estimated in-situ to adequately predict mixing and transport of substances in the estuarine water. This chapter describes and summarizes previous research works on estimating the dispersion coefficient.

2.1. Dispersion studies

Several studies had been conducted to estimate dispersion coefficient with the purpose of studying hydrodynamics, salinity intrusion or predicting fate and transport of pollutants in estuaries.

James River, Virginia – Pritchard (1950)

In 1950, extensive measurements were undertaken in the James River estuary by averaging measured data over one or more tidal cycles. The section of the estuary investigated was delineated between 20 and 45 Km above the mouth of the river, and a number of sampling stations were operated for three periods with a minimum sampling period of four days during which serial measurements of tidal current, salinity and temperature were taken. (Dyer, 1997)

During this study, it was observed that the low water/ebb-cycle salinities were noticeably lower than the high water/flood-cycle values, and in some cases having concentrations at high water about 4 times higher than those at low water (Fig. 2.1). With respect to the velocity measurements, the cross-sectional mean value of the horizontal diffusive flow was calculated as less than 5% of the mean flow, indicative of a dominant advective tidal transport characteristic.

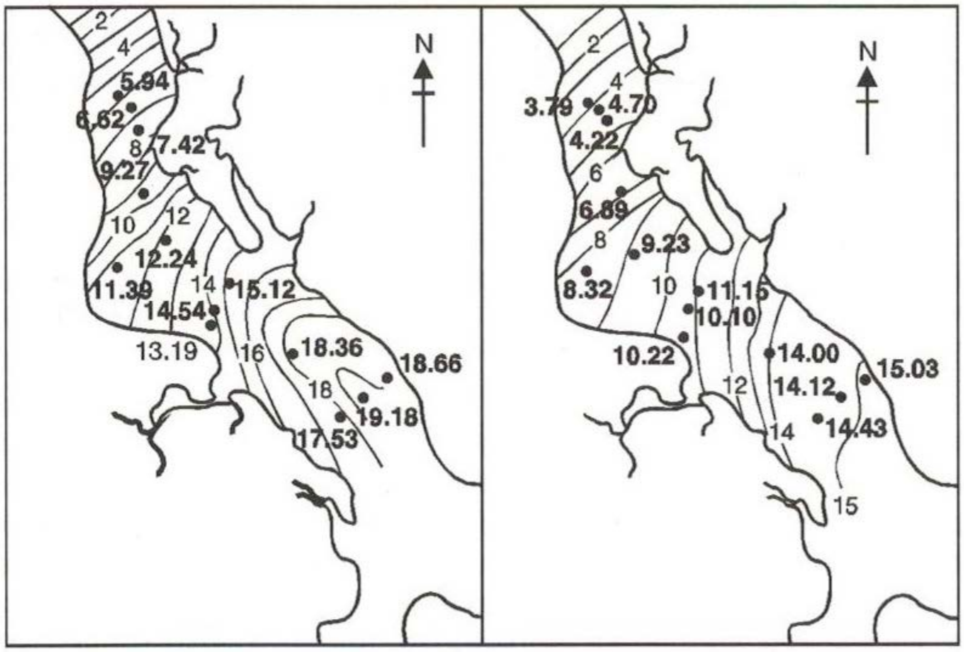

Fig. 2.1. Salinity distribution in the lower James. Left hand, high water; right hand, low water. (Dyer, 1997)

The main purpose of Pritchard's study was to investigate the salt balance and the advective and diffusive properties in the lower reach of the James River estuary. The final outcome revealed that the salt flux rises with the tidal velocities, and the horizontal advective term and the vertical non-advective term (turbulent) term were most dominant in the study area, with the vertical advective term becoming important at mid-depth near the halocline. Reported value of vertical Eddy diffusion coefficient K_z was 9 cm^2/s.

Duwamish River, WA – Hugo Fischer (1965)

In 1965, Fischer carried out a research in the tidal Duwamish River, WA, at the upstream reach of the point of discharge from the Renton Sewage Treatment Plant (today known as King County South Treatment Plant). The purpose of this study was to provide an exact description of the movement and dispersion of the sewage effluent introduced in the study reach and to make a detailed investigation of the basic mechanics of dispersion in a natural environment.

The study consisted in four trials of longitudinal dispersion experiments in which a dye (Rhodamine B) was injected upstream from the study reach with a series of observation stations established at downstream sections throughout the reach. Dye concentrations were measured and aerial photographs were taken over two consecutive days.

Two different methods of predicting dispersion coefficients were employed in Fischer's study; Integration of Taylor equilibrium profile and Numerical analysis. Integration of Taylor equilibrium profile is to determine diffusive transport by applying the conservation of mass equation:

$$\frac{\partial c}{\partial t} + u\frac{\partial c}{\partial x} = \frac{\partial}{\partial y}E_y\frac{\partial c}{\partial y} + \frac{\partial}{\partial z}E_z\frac{\partial c}{\partial z} \qquad \text{Eq. (2.1)}$$

where

c = Concentration at a point

u = Velocity at a point, in the *x* direction

x = Coordinate in the longitudinal direction

y = Coordinate in the vertical direction

z = Coordinate in the lateral direction

E_y = Turbulent diffusion coefficient in the *y* direction

E_z = Turbulent diffusion coefficient in the *z* direction

From lateral variations in dye concentrations, experimental values of E_z were calculated with a numerical integration of the mass balance equation from which values of dispersion coefficient were obtained.

In Numerical analysis approach, computers were used to solve a step-by-step simulation of the physical process, where the total flow was divided by vertical lines into n cylindrical stream tubes of area A_1, A_2… A_n, with $n \le 10$ (Fig. 2.2.) to capture variations in lateral and vertical directions. Each stream tube then was assigned with a velocity value obtained from actual measurements.

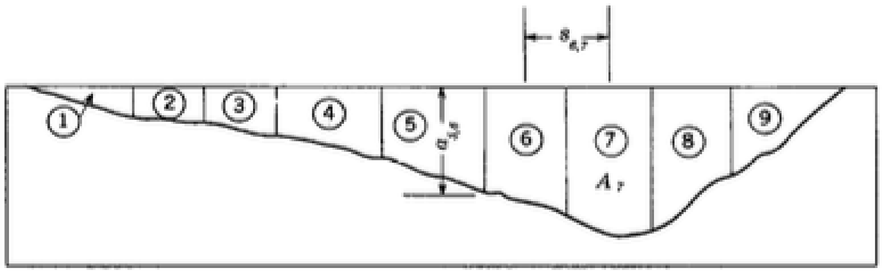

Fig. 2.2. Division of flow into stream tubes. (Fischer, 1965)

Findings of this study revealed significant tidal influence over dye concentration at river segments adjacent to the estuary, whereas in the most upstream locations, river segments behave as a normal uni-directional river, with the dispersion influenced largely by the bed friction.

Dispersion coefficient estimates from two methods were very close to the estimates calculated from the dye study field data that validated the application of both Integration of Taylor equilibrium profile and Numerical analysis methods. It was also found that the accuracy of the Numerical analysis method is constrained to; a) uniform channel geometry and b) larger measurement points in the cross section to accurately capture variations in dye concentration.

<u>James River, VA at the Nansemond River mouth – Albert Kuo (1974)</u>

In the Hampton Roads area of Virginia, the Virginia Institute of Marine Science (VIMS) have conducted dye studies to evaluate dispersion and transport of pollutants in the James and the Rappahannock River During the summer of 1974, Kuo, A. and Jacobson, J.P. developed a method for predicting the concentration distribution of a sewage constituent in the James River from a location where a sewage outfall of the Nansemond Sewage Treatment Plant was proposed. In their study, Rhodamine WT day was use to conducted two dye studies to simulate release of pollutants during flood and ebb cycles.

A number of assumptions used in the study include; a) due to the shallow water depth (in comparison to the horizontal dimensions) of the water body at the study site, the vertical variation of water constituents outside of the initial mixing zone is considered as negligible compared to the horizontal variations, and b) water quality problem is severe due to a weak density stratification occurred during summer time.

Two separate releases of the dye and subsequent mixing and transport were monitored for a period of four days in each dye study. Two moving boats equipped with flow-through fluorometers and navigation units traversed the study area at slack waters before ebb and flood. Collected data were transferred to a chart of the area and contours of equal dye concentration were drawn yet the study did not estimate resultant dispersion coefficients.

It was observed that the initial plume at the first Slack before Flood (SBF) was narrow and long (about 6 miles long and less than 1 mile wide); at the following Slack Before Ebb (SBE), the dye cloud reached from shore to shore and dispersed over broad areas with several patches. At the second SBF the dye cloud further dispersed and moved downriver. By the fourth SBF the dye dispersed over a large area and much of the dye left the James and went into the Chesapeake Bay. The observations of dye concentration distribution clearly show the effects of advective transport occurred at SBF and its subsequent dispersive transport between SBF and SBE, where the salinity intrusion of the flood cycle increase the dispersive movement of dye concentrations over the area of study. The SBE and SBF were selected as they are the extremes of the tidal excursion and therefore the most significant periods to identify variations of concentration fields with phase of tide. Goal of the study was to predict the distribution of the concentration of the parameters of interest, Residual Chlorine in particular concern for possible adverse effects over oyster and clam larvae.

<u>Rappahannock River, VA – Anne Catherine Wilber (1986)</u>

The Rappahannock River, a partially-mixed estuary in the Virginia coastal plain, was simulated with a real-time, hydrodynamic and salinity intrusion model based on the one-dimensional equation of conservation of volume, momentum and mass.

Applying finite difference scheme, the estuary was divided into 44 unequal segments by locating 45 transects from the fall line to the mouth of the Chesapeake Bay. In Wilber's study, estimation of dispersion coefficient was formulated by applying three dispersion terms to reflect following effects:

- Effect of vertical shear of the tidal flow
- Effect of transverse shear of the tidal flow
- Effects of gravitational circulation

The first two terms were applied in the freshwater portion of the estuary where dispersion coefficient accounts for the longitudinal mixing due to turbulent diffusion and shear induced velocity distribution in the transverse and vertical directions. The last term was applied to the saline portion of the estuary where the effect of gravitational circulation depends on the salinity gradient.

The model was then calibrated for hydrodynamic parameters and longitudinal salinity distribution intrusion using the field data obtained from an intensive survey conducted on the lower Rappahannock during July 30 and 31 1973 (spring tide period) at slack water. Model estimates were then compared with the field data, and results indicated that the predicted currents were lower than the measured due to predictions made for average current speed while field measurements were taken in the channel, where speeds were the highest.

For longitudinal salinity distribution, the model estimates were accurate for a wide range of freshwater inflow rates; however, in the middle of the salinity intrusion region, the predicted salinities were lower than the measured while in the inner region of the intrusion the predicted values were higher, indicative of complex mixing mechanisms in saline region of the river.

Study concluded that by incorporating the effect of gravitational circulation in the saline portion of the estuary, dispersion coefficient can be more accurately predicted, given that the dispersion due to of gravitational circulation effect is several orders of magnitude larger than due to the shear flow. On the other hand, shear flow was the prime source of dispersion in the freshwater portion of the estuary where the current speed was greatest.

Sumjin River, Korea – Shana *et al.*, (2011)

Three years of hydrographic data taken at low and high tides along with the main longitudinal axis of the Sumjin River Estuary (SRE) in Korea were used to estimate the spatial and temporal variation of the effective longitudinal dispersion coefficient.

In addition to the longitudinal dispersion coefficient estimation, the effects of freshwater discharge, tidal height and salinity gradient corresponding to the spatially varying longitudinal dispersion coefficient were examined.

In this research, twenty-five (25) conductivity-temperature-depth (CTD) sensors were installed per monitoring station replicated in a 1 km resolution along the saline intrusion portion of the estuary. Subsequently, a total of 24 longitudinal salinity transects were obtained at low and high tide during spring tide in each season from August 2004 to April 2007.

To determine the longitudinal dispersion coefficient, the author applied the salt balance equation, integrated with respect to x (Savenije, 1986; 1989; 2005) with equilibrium between advective and dispersive fluxes under tidal average conditions:

$$D_i(x) = \frac{QS_i(x) / A_i(x)}{\frac{\partial S_i}{\partial x}} \qquad \text{Eq. (2.2)}$$

The numerator in Eq. (2.2) represents the advective rate of transport of salt seawards by the river flow, Q per unit area of cross-section, A(x) and the denominator represents the longitudinal salinity gradient.

The results indicated that the range of the dispersion coefficient was rather broad at high water slack (HWS) (values varied between 100 and 494 m^2/s) and narrower at low water slack (LWS) due to different tidal amplitudes. The spatially varying dispersion coefficient had maximal values (> 300 m^2/s) near the mouth at high water, and decreased gradually toward upstream with fluctuations. The temporally varying dispersion coefficients were positively correlated with river discharges at both low and high tide, where the estimated values increased with increasing river discharge and decreased with diminishing river discharges.

CHAPTER 3.

STUDY SITE

Study site locates in the partially-mixed lower reach of the James river estuary in Virginia; a tidal section at approximately 19 miles upstream from the mouth at the Chesapeake Bay, in the City of Newport News. The area comprises approximately 330,000 m^2 (longitude: 1100 m, width: 300 m) along the shore in the merging point of the Warwick River and the James River. The area is surrounded by a recreational park, a residential area and a wastewater treatment plant (James River Wastewater Treatment Plant).

Study area was selected with the purpose of characterizing area's mixing and transport of substances by advective and dispersive processes in a tidal estuarine body of water.

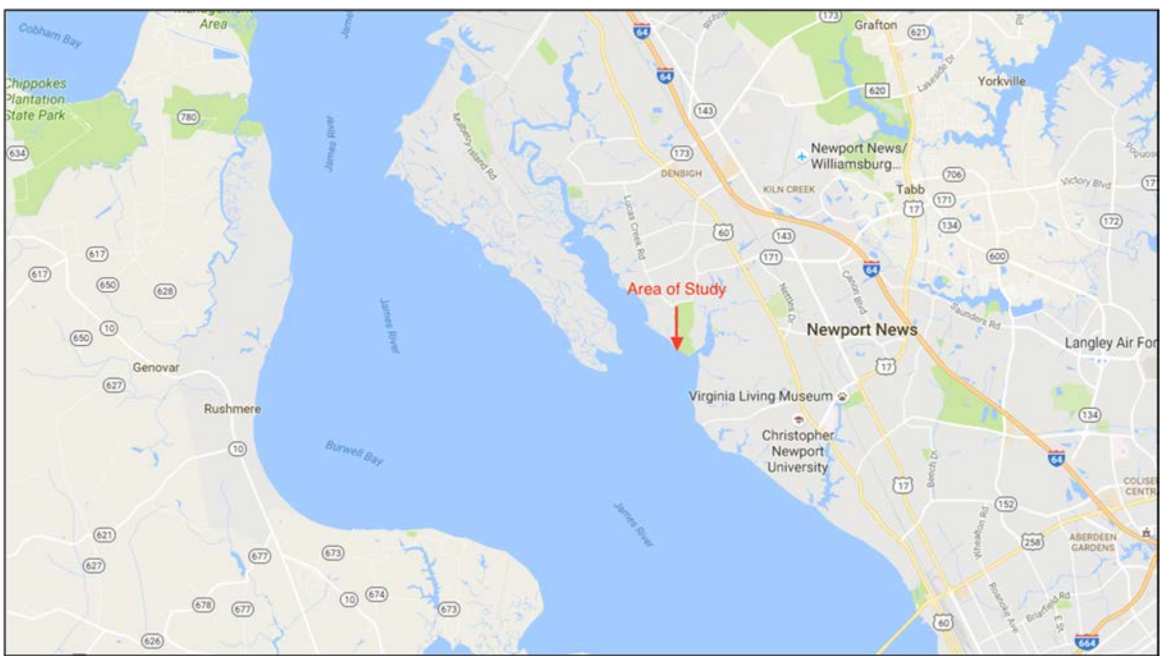

Fig. 3.1. Map of Area of Study

Although the James River has been subject to diverse source of pollutions along its 340 miles length and subsequently many water quality studies had been carried out for estimating the amount of nutrient loading into the Chesapeake Bay, there is no previous studies of dispersion coefficient estimation, or substance mixing and transport characterization performed in this particular area of the river, with an exception of the study developed by Pritchard back in 1950 in a low-resolution, meso-scale effort.

In the study area, the James River receives the inflow of the Warwick River, a 14-mile-long body of water surrounded by residential and commercial areas of York County, the City of Newport News and the Fort Eustis U.S. Army base. Due to the high population density along its watershed, there are multiple nonpoint sources of pollution mainly associated to wildlife, grazing livestock, urban/suburban runoff, failed and malfunctioning septic systems, and uncontrolled discharges (DEQ, 2007) that drain directly into the Warwick River or its tributaries such as Lucas Creek, Stoney Run Creek and Deep Creek.

The only reported point source of pollution in the study area is the James River Wastewater Treatment Plant effluent whose submerged 60” and 48” diameter outfall pipes extend about 0.7 miles from the shore line that is configured with a 48” and 30” diffusers (Figure 3.2.).

Reported amount of TSS discharged by the plant during the two days of in-situ sampling (July 21st and 22nd 2016) conducted in this study was an average value of 1.3 mg/L at 12.46 MGD of flow, for a total loading of 0.061 Kg/d. With measured field sampling data, this study focuses in characterizing mixing and transport mechanisms of Total Suspended Solids in the River including the effect of TTS influx from the James River Wastewater Treatment Plant effluent discharge.

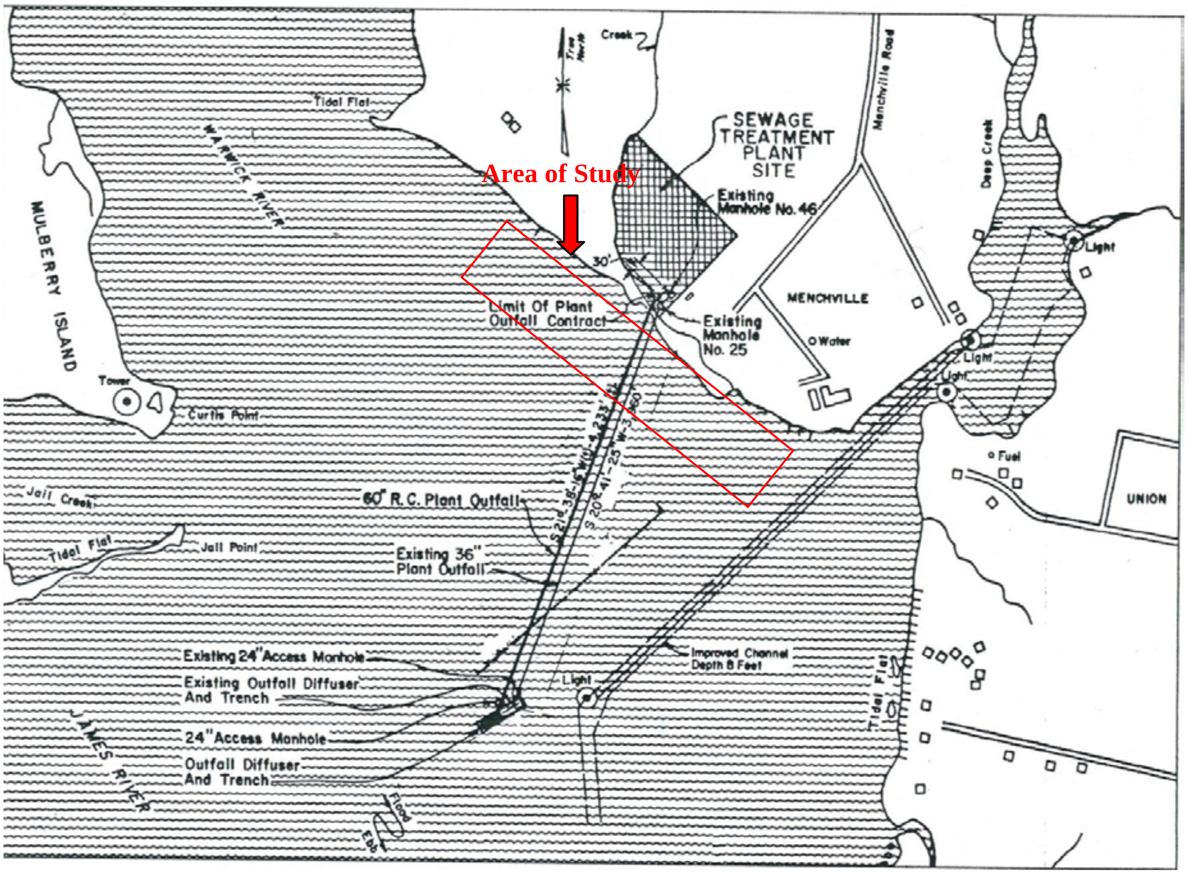

Fig. 3.2. HRSD James River Plant Outfall – Source: HRSD

CHAPTER 4.

METHODOLOGY

4.1. Assumptions and Limitations

Estuaries are dynamic bodies of water with very complex hydromorphology and hydrodynamics, highly influenced by atmospheric processes, river discharge and salinity intrusion, it is critical to evaluate those site-specific factors to characterize and accurately predict mixing and transport phenomena.

The main objectives of this study are to use in-situ salinity concentrations to estimate the longitudinal dispersion coefficient, and consequently perform a characterization of Total Suspended Solids mixing and transport mechanisms over a tidal section of the James River, evaluating the influence of advective and dispersive processes.

4.1.1. Total Suspended Solids and Turbidity relationship

Total Suspended Solids and Turbidity are parameters used to evaluate clarity of water contributed by organic and inorganic matters. Both parameters are directly influenced by runoff, industrial, domestic wastewater discharge, aerial deposition and resuspension processes.

Major difference between TSS and turbidity is that TSS is a measurable, mass-quantitative parameter whereas turbidity is a relative, qualitative parameter. Estimation of TSS requires a lengthy and tedious laboratory process whereas turbidity measurement can be obtained instantaneously. As a result, turbidity is far more frequently used for describing level of water clarity.

In this study, to obviate time consuming method required for determining Total Suspended Solids concentrations, a site-specific General Linear Model (GLM) was developed by utilizing 15-year TSS/Turbidity data series for the effluent discharge from the James River Treatment Plant. Resultant GLM was then used to synthesize TSS as the dependent variable with an independent variable of field measured turbidity from the study site. Estimated TSS data were used subsequently in Finite Segment Method (FSM) and the Steady State Response Matrix (SSRM) to characterize the Total Suspended Solids mixing and transport in the study area.

Following General Linear Model (GLM) analysis procedure was implemented for this study to develop an in-situ relationship between Turbidity and TSS.

Univariate Procedure – Extreme Outliers identification:

From 15-year TSS/Turbidity data series for the effluent discharge from the James River Treatment Plant, data distribution, statistical parameters and outliers from the entire data set of the dependent variable (TSS) were analyzed by using the Univariate procedure in the Statistical Analysis System (SAS) software. Extreme TSS outliers beyond 3*Interquartile Range (IQR) were identified and screened to prepare a TSS/Turbidity model data series which has 3832 data pair observations. The extreme outliers were identified as any value equal or greater than 27.3 mg/L of TSS.

Univariate procedure – Normality test:

Normality test was a necessary procedure to determine if the dependent variable (TSS) is normally distributed and therefore applicable to General Linear Model (GLM). TSS/Turbidity model data series of 3832 observations were examined with Kolmogorov-Smirnov (K-S) test at alpha=0.05 significance in the Univariate procedure, SAS. *p*-value from K-S test was less than 0.05, indicative of non-normality of the dependent variable, TSS. Alternatively, using a larger sample size condition, Central Limit Theorem was applied to the dependent variable, TSS, as approximately normally distributed for further analysis.

General Linear Model procedure – Least-Square Regression Analysis (with Intercept suppressed):

General Linear Model (GLM) development for the TSS and Turbidity relationship was the final step to determine if a real correlation between the two parameters existed. The linear least-square regression method with intercept suppression at alpha=0.05 was used for the 3832 Paired observations. Results showed that the proposed least-square model was valid (p-value < 0.05), indicating a contributing relationship between independent variable, turbidity and dependent variable, TSS. Estimated model performance was also evaluated with f_0 ratio (=MSR/MSE), which was greater than 25.

General form of the least-square regression model is expressed as;

$$\hat{y} = \hat{\beta}_0 + \hat{\beta}_1 x \quad \text{(with intercept)} \qquad \text{Eq. (4.1)}$$

$$\hat{y} = \hat{\beta}_1 x \quad \text{(with intercept suppressed)} \qquad \text{Eq. (4.2)}$$

where
$\hat{y}$ = Dependent variable (TSS)
x = Independent variable (Turbidity)
$\hat{\beta}_0$ = Intercept
$\hat{\beta}_1$ = Regressor coefficient

Once estimated, estimated regression model validity is tested with a test of hypothesis on the correlation between the dependent and the independent variable:

H_0: $\hat{\beta}_i = 0$

H_a: At least one $\hat{\beta}_i \neq 0$

where $\hat{\beta}_i$ represents the estimated regressors.

The null hypothesis H_0, with a 95% level of confidence, tests if none of the independent variables or regressors is correlated to the dependent variable. For this evaluation, two scenarios were possible:

1. Rejection of Null Hypothesis (If p value is less than α = 0.05). In this case, the alternative hypothesis (H_a) becomes the final conclusion of the test that with a 95% level of confidence there is an insufficient evidence indicating that all regressors coefficients are zero; therefore, it will be highly likely that at least one or more regressors is different than zero, which means that there is a relationship between dependent and independent variable.

2. Non-Rejection of Null Hypothesis (If p value is equal to or greater than α = 0.05). In this case we conclude that with a 95% level of confidence there is sufficient evidence indicating that that all regressors are zero, indicating no correlation between dependent and independent variables.

Table 4.1. Test of Hypothesis results

	P value	F Value	R^2
Hypothesis 1 (Normality Test)	<0.0100		
Conclusion	with a 95% level of confidence there is insufficient evidence indicating that the TSS data came from a normally distributed system. Alternatively, Central Limit Theorem was applied to assume normality.		
Hypothesis 2 (Linear Regression)	<0.0100	54073.1	0.9338
Conclusion	with a 95% level of confidence there is insufficient evidence indicating that all regressors coefficients are zero; therefore, it will be highly likely that at least one or more of the regressors is different than zero, which means that there is a relationship between dependent and independent variable.	Good model performance (F>25)	93.38% of the data is represented in the regression analysis

The statistical analysis carried out by using the data set of Total Suspended Solids and turbidity from the effluent discharge of a wastewater treatment plant indicated a valid correlation between these two parameters (p-value < 0.05), providing sufficient evidence at 95% level of confidence indicating that TSS and Turbidity had a linear relationship. Estimated model performance was also evaluated with f_0 ratio (=MSR/MSE), which was greater than 25. (Appendix IV shows the SAS outputs).

Estimated General Linear Model (GLM) to the site-specific to study area is expressed as;

$$TSS\ (\frac{mg}{L}) = 1.71487 * Turbidity \qquad \text{Eq. (4.3)}$$

Equation 4.3 will be valid over a TSS range between 1.5 mg/L and 27.5 mg/L according with the results of the Histogram.

4.1.2. Steady State Assumption and two-dimensional approach

Although some estuaries may never be considered as steady-state systems due to continuous weather influences contributing to river flow, tidal ranges and sediment distribution; this study will assume general steady state conditions of flow and tidal characteristic at study site.

Estuaries water quality studies generally consider two-dimensional models due to the sufficiently large width of estuaries where variations in longitudinal and transversal directions are considered more influential than vertical changes in salinity gradients. The relative shallowness in the section of the river in the study area is the rationale to apply a two-dimensional approach in modeling TSS mixing and transport mechanisms. According with Wo-Seng Long (1993), there are two dimensional vertically averaged hydrodynamic models for water quality estimation:

- Intratidal calculations: Where the tidal flows are explicitly taken into account. This approach is appropriated for the detailed description of the distribution that results from highly time-variable inputs of mass such as a spill or a storm water overflow.

- Intertidal calculations: Where only the net, non tidal flows are considered. This model is more appropriate for the seasonal time scale that characterizes the intratidal hydrodynamic model calculations averaged over the tidal cycle in order to produce the net non-tidal flow distribution.

This study considered the Intertidal calculations approach that the TSS concentrations per segment are evaluated, applying average values of the two tidal cycles evaluated, and then comparing them with the concentrations obtained per flood and ebb cycles for a posterior verification.

4.1.3. Data requirements

Estuarine data collection requires simultaneous sampling at several locations and time intervals over a complete tidal cycle. The data collection usually involves collecting in-situ data such as water depth, velocity, salinity, temperature, water quality, pollutants loading, freshwater flow and the estimation of dispersion, reareation, settling, etc.

Where lateral or vertical mixing is strong, centre-line data or depth averaged data may be sufficient to represent water quality characteristics, and therefore the amount of cross sections needed can be reduced considerably. The data are usually collected in the summer with low freshwater flow and at maximum temperature, that should theoretically represent the “worst” condition for the water quality in the estuary. If water quality objectives can be satisfied at this time of the year, then they can usually be achieved through the year (Rinaldi *et al.*, 1979).

4.2 Methods

4.2.1. Finite Segment Method

The finite segment method is a technique that signifies and evaluates partial differential equations in the form of algebraic equations. Values are calculated at discrete places on a meshed geometry. “Finite segment” refers to the small segment surrounding each node point on a mesh. In the finite segment method, volume integrals in a partial differential equation that contain a divergence term are converted to surface integrals, using the diverge theorem. These terms are then evaluated as fluxes at the surface of each finite segment. (Miller, E.G., 1960).

It is assumed in the 2-D finite segment model that each segment is completely mixed as a CMFR (Completely Mixed Flow Reactor). Therefore the concentration gradient occurs only along the x- and y-axes over subsequent and adjacent segments, and the concentration gradient in the z-axis would be negligible. Since the segment topography is reflected to satisfy an equal steady-state volume in segment series, FSM is an ideal application to simulate estuaries with complex bottom topography without any difficulty. (Thomann, R.V., 1983).

Then FSM uses the mass balance among segments by accounting for and calculating mass transport due to advection, dispersion, loading and decay over time. This procedure is referred to as Compartmentalization and interchange between compartments is simulated via bulk dispersion as shown in Figure 4-1. The assumption of complete mixing reduces the set of partial differential equations to ordinary differential equations (Schnoor, 1996).

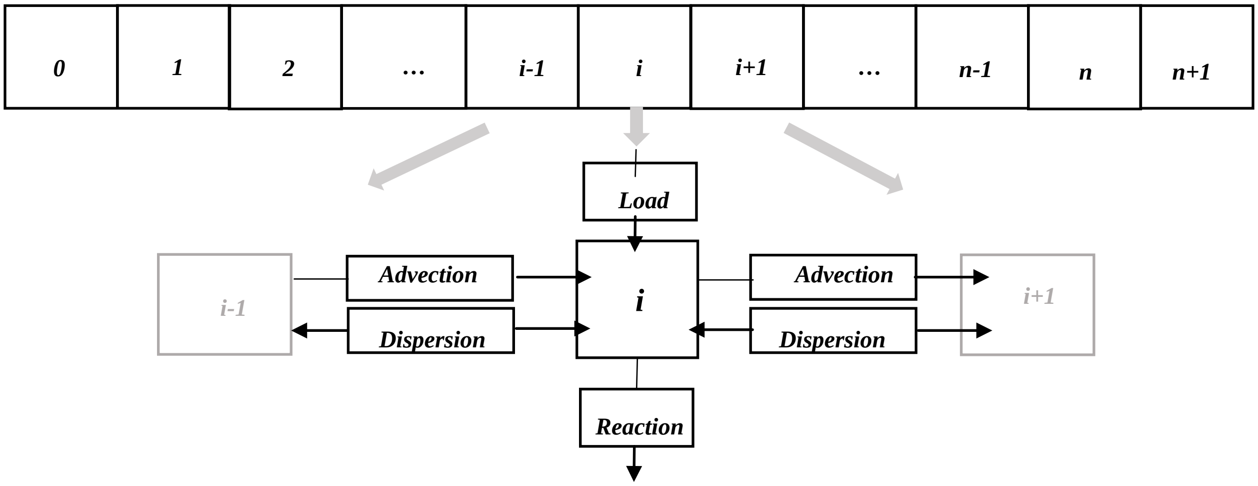

Figure 4.1. Compartmentalization used in Finite Segment Method

Compartmentalization is based on dividing the water body into "control volumes" assuming the complete mixed flow in each segment and identical volumes. The segment *0* and *n+1* represent boundary segments and therefore there will be *n* unknowns with a system of *n* equations. (Chapra, 2008). Then subsequent finite Segment Model is developed from the following second-order differential flux equations (Thomann and Muller, 1997).

$$V\frac{\partial C}{\partial t} = -Q\frac{\partial C}{\partial x}\Delta x - \Delta QC + \frac{\partial}{\partial x}\left(EA\frac{\partial C}{\partial x}\right)\Delta x - kCV$$
$$V\frac{\partial C}{\partial t} = -Q\frac{\partial C}{\partial y}\Delta y - \Delta QC + \frac{\partial}{\partial y}\left(EA\frac{\partial C}{\partial y}\right)\Delta y - kCV \qquad \text{Eq. (4.4)}$$

where C represents the concentration of Total Suspended Solids present on each segment, E is the dispersion coefficient, and k is the kinetic reaction constant. This flux relationship can be further expressed to reflect spatial invariant flow/discharges and dispersion coefficients in the segments (Thomann and Muller, 1997).

$$\frac{dC}{dt} = E_x\frac{d^2C}{dx^2} - U\frac{dC}{dx} - kC$$

$$\frac{dC}{dt} = E_y \frac{d^2C}{dy^2} - U\frac{dC}{dy} - kC \qquad \text{Eq. (4.5)}$$

With control volume and steady state assumption, the mass balance in a finite segmental expression becomes:

$$0 = W_i + Q_{i-1,i}c_{i-1} - Q_{i,i+1}c_i + E'_{i-1,i}(c_{i-1} - c_i) + E'_{i,i+1}(c_{i+1} - c_i) - k_{si}V_i c_i \qquad \text{Eq. (4.6)}$$

where

W_i = Loading on segment i

$Q_{i-1,i}$ = Flow from segment i-1 to segment i

$Q_{i,i+1}$ = Flow from segment i to segment i+1

c_{i-1} = Concentration at the segment i-1

c_{i+1} = Concentration at the segment i+1

c_i = Concentration at segment i

$E'_{i-1,i}$ = Bulk dispersion coefficient between segments i-1 and i

$E'_{i,i+1}$ = Bulk dispersion coefficient between segments i and i+1

k_{si} = First order settling rate constant for segment i

V_i = Volume of segment i

This equation considers n equations with $n+2$ unknowns (c_0 through c_{n+1}). Therefore, the Dirichlet boundary conditions are applied to specify the concentration at the boundary.

A series of simultaneous equations will produce a matrix referred to as Steady State Response Matrix (SSRM) from which the mechanisms of Total Suspended Solids transport per each of the evaluated segments will be analyzed:

$$(-Q_{i-1,i} - E'_{i-1,i})c_{i-1} + (Q_{i,i+1} + E'_{i-1,i} + E'_{i,i+1} + k_{si}V_i)\, c_i + \left(-E'_{i,i+1}\right)c_{i+1} = W_i \qquad \text{Eq. (4.7)}$$

The n number of simultaneous equations can be written in matrix form:

$$[A]_{nxn} \text{ x } [c]_{nx1} = [W]_{nx1} \qquad \text{Eq. (4.8)}$$

where A represents the matrix coefficients, c is the matrix of unknowns and represents the concentration of Total Suspended Solids in each segment affected by transport from to nearby segments, and W is the internal loading matrix which shows the existing values of TSS in each segment

To determine the resultant concentration of TSS in each segment, the linear equations needs to be solved simultaneously

$$[c]_{nx1} = [A]_{nxn}^{-1} \text{ x } [W]_{nx1} \qquad \text{Eq. (4.9)}$$

4.2.2. Constant Segment Volume for Finite Segment Method

Segmentation of the study area included 10 segments of equal volume (5 segments longitudinal to the shore line and 5 segments in lateral configuration) as shown in Figure 4-2a. Initial proposed segment configuration included only 8 segments to evaluate mixing and transport of TSS from a point source (discharge of James River treatment plant). However, after further analysis of the field data and information obtained from HRSD about the effluent discharge, it was determined the need of adding two additional segments that would act as boundary conditions in the row of existing segments 6,7 and 8. These new segments were labeled as segment 1' and segment 5' and are transversal to the shoreline.

Initial configuration of segments

Segmental length and width (200 m) were selected to be extensive enough to collect at least three salinity samples within segment and to cover enough width to be out of shore as shown in Figure 4-2b. The volume of each segment was calculated with the purpose of identifying and selecting the smallest value as the control volume. Using the bathymetry information, the longitudinal cross sectional area between segments is calculated as trapezoidal area with D1 being the depth facing shore and D2 the depth toward the center of the River

Figure 4-2a. Segments configuration

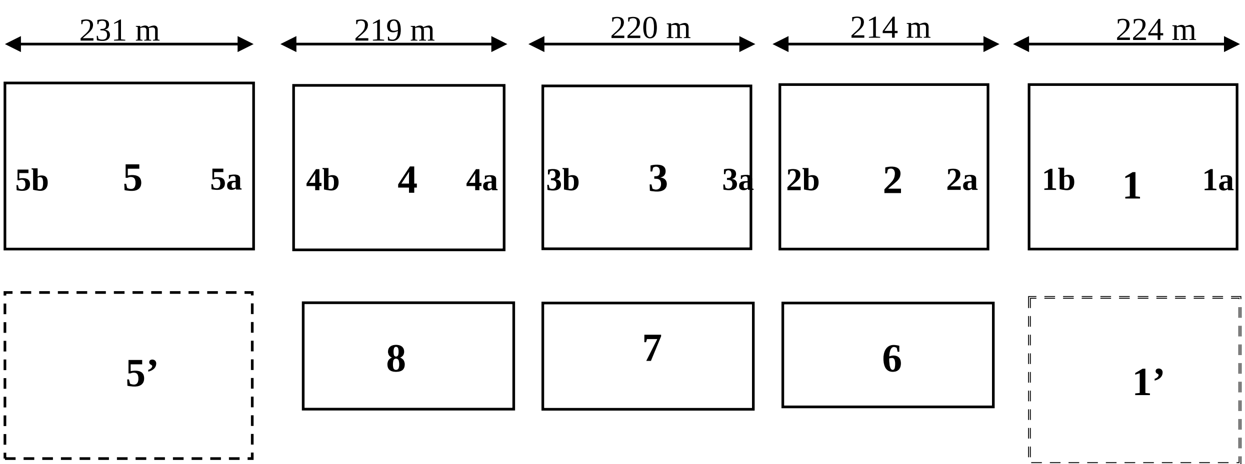

Figure 4-2b. Segmental Dimension and Sampling Locations

Table 4.2. Initial segments configuration

Segment	L (m)	W(m)	D1 (m)	D2 (m)	Cross Sectional Area (m^2)	Volume (m^3)
1	224	200	0.3	0.6	90	20160
1’	224	200	0.3	0.6	180	40320
2	214	200	0.3	0.6	90	19260
3	220	200	0.3	0.6	90	19800
4	219	200	0.3	0.6	90	19710
5	231	200	0.3	0.6	90	20790
5’	231	200	0.3	0.6	180	41580
6	214	200	0.6	1.2	180	38520
7	220	200	0.6	1.2	180	39600
8	219	200	0.6	1.2	180	39420

From the calculated volumes, segment 2 volume is selected as the control volume: 19260 m^3. With the control volume, it was necessary to determine the longitudinal interface area between segments to then calculate the width from the shore to the center of the river that allowed the segments to have the same volume to apply the Finite Segment Method. The resultant segments dimensions are shown in Table 4.5.

4.3. Procedures and Calculations

4.3.1. Data Collection

In-situ data collections were carried out during Thursday July 21st and Friday July 22nd of 2016 at the eight selected locations (five along the shore and three parallel to the three centered segments in direction towards the center of the river) based on site accessibility, known bathymetry and proximity with the point source discharge of the James River Treatment Plant. It was necessary to consider the collection of at least three values of salinity per segment in order to compute an individual dispersion coefficient for each segment, and calculate TSS transport in 2-D.

For the additional two segments (1’ and 5’) added as boundary conditions, since no data was collected during the surveys of July 21st and 22nd, it was assumed that the salinity and velocity concentrations were equivalent of segments 1 and 5 respectively. However, concentrations of TSS for these two boundaries were taken from the latest report of the nearest

James River Station (LE.5.2.). The TSS concentration for August 13 2015 was 11 mg/L. Location of Station LE.5.2 is shown in Figures 4.3a and 4.3b.

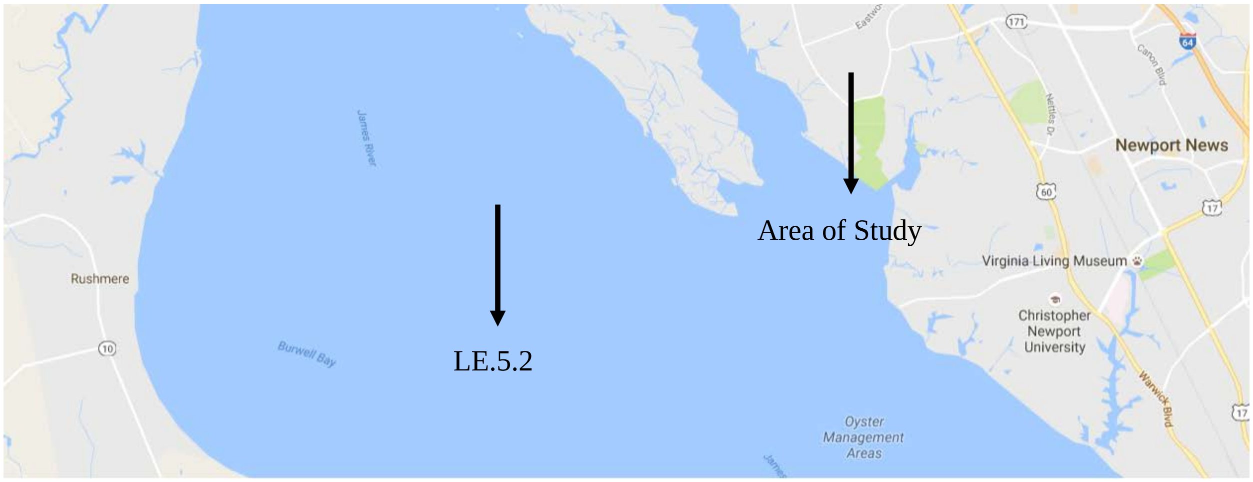

Figure. 4.3a. Location of monitoring station LE.5.2.

Figure. 4.3b. Location of monitoring station LE.5.2.

4.3.1.1. Salinity, Turbidity and velocity

Salinity concentrations, turbidity and velocity were sampled on-site. Salinity concentrations were measured using the Sper Scientific salinity probe model 850048C/S with 0.01 ppt resolution (up to 10 ppt). Turbidity values were measured using Sper Scientific turbidity meter model LUTU-2016 with 0.01 NTU resolution between 0-50 NTU. The results are summarized in Tables 4.3 and 4.4

Table 4.3. In situ data July 21st
Water Temperature a.m.: 27 C – Water Temperature p.m.: 28 C

Point/ Segment	Segment Length (m)	Salinity (ppt)		Turbidity (NTU)		Velocity (m/s)	
		10:00 a.m.	4:00 p.m.	10:00 a.m.	4:00 p.m.	10:00 a.m.	4:00 p.m.
1a		8.86	8.09	6.98	6.74		
1	224	8.64	8.06	8.02	6.19	0.15	0.22
1b/2a		8.81	8.01	7.94	7.16		
2	214	8.76	7.93	8.67	9.53	0.15	0.32
2b/3a		8.65	7.91	7.08	8.15		
3	220	8.63	7.89	8.47	6.93	0.19	0.13
3b/4a		8.58	7.82	8.22	5.51		
4	219	8.53	7.77	5.95	5.82	0.12	0.29
4b/5a		8.51	7.73	9.89	5.14		
5	231	8.48	7.71	9.24	9.83	0.15	0.46
5b		8.47	7.6	10.83	7.91		
6	214	8.73	8.16	5.23	10.29	0.22	0.3
7	220	8.67	8.05	5.44	8.74	0.3	0.55
8	219	8.66	7.78	5.89	5.81	0.14	0.13

Table 4.4. In situ data July 22nd
Water Temperature a.m.: 28 C – Water Temperature p.m.: 30 C

Point/Segment	Segment Length (m)	Salinity (ppt)		Turbidity (NTU)		Velocity (m/s)	
		10:00 a.m.	4:00 p.m.	10:00 a.m.	4:00 p.m.	10:00 a.m.	4:00 p.m.
1a		9.21	7.94	28.11	14.7		
1	224	9.18	7.85	24.8	9.47	0.22	0.14
1b/2a		9.17	7.82	17.79	9.23		
2	214	9.21	7.94	22.03	24.69	0.23	0.21
2b/3a		9.41	7.77	36.47	45.26		
3	220	9.25	7.76	22.82	13.48	0.15	0.23
3b/4a		9.19	7.64	18.55	11.74		
4	219	9.25	7.59	12.91	15.67	0.22	0.25
4b/5a		9.29	7.58	8.56	6.66		
5	231	9.26	7.57	13.54	13.47	0.21	0.14
5b		9.25	7.54	11.47	10.51		
6	214	9.29	7.92	17.82	7.45	0.23	0.28
7	220	9.27	7.71	13.74	9.61	0.23	0.4
8	219	9.31	7.58	14.78	10.85	0.21	0.24

4.3.1.2. Bathymetry

Bathymetry in the study area was obtained from NOAA (National Oceanic and Atmospheric Administration) Nautical charts (NOAA Chart 12248), and was used for calculating the cross-sectional areas of the segments evaluated. NOAA Chart 12248 is shown in Figure 4.4.

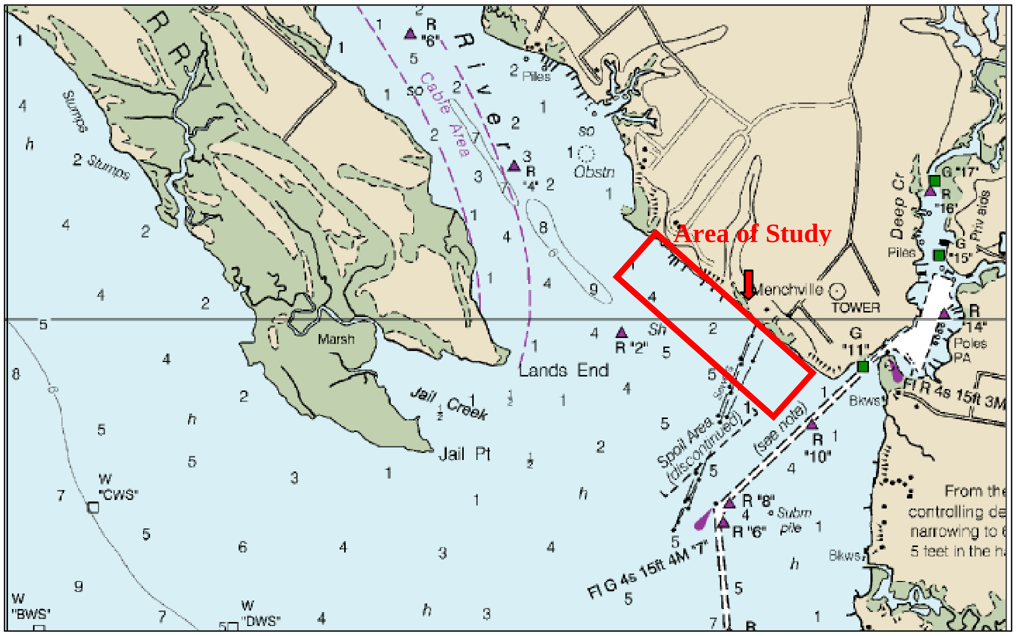

Figure 4.4. Bathymetry of the Study Area (NOAA Chart 12248)

Bathymetry data was used in estimating the cross sectional area of each studied segment from the control volume. With the cross sectional area, the final length of each segment was calculated:

<u>Segment 1</u>

A_1 = Initial area calculated (trapezoid)

$A_1 = \frac{B1+B2}{2} * W$

$A_1 = \frac{0.6m+0.3m}{2} * 200m$

$A_1 = 90\ m^2$

A_1' = Available area

$A_1' = V/L$

L = Segment length

$A_1' = 19260\ m^3/224\ m$

$A_1' = 85.98\ m^2$ (available area)

W_1 = Initial estimated width of segment = 200 m

W_1' = Calculated width of segment

$$\frac{A_1}{A_1'} = \frac{W_1}{W_1'}$$

Substituting: A_1, A_1' and W_1, we have: $W_{1'}$ = 191 m

The same approach was used to determine the length of remaining segments. Table 4.5. shows the final segmental dimension used in the Finite Segment Method in this study:

Table 4.5. Final Segmental Dimension Used in the Finite Segment Method

Segment	**A_1(m^2)**	**A_1' (m^2)**	**W_1 (m)**	**W_1' (m)**	**L (m)**	**Volume (m^3)**
1	90	85.98	200	191	224	19259
1’	180	85.98	200	95.5	224	19259
2	90	90	200	200	214	19260
3	90	87.54	200	194	220	19259
4	90	87.95	200	195	219	19261
5	90	83.38	200	185	231	19261
5’	180	83.38	200	92.5	231	19261
6	180	90	200	100	214	19260
7	180	87.54	200	97	220	19259
8	180	87.95	200	97.5	219	19261

4.3.1.3. Wind Speed

Wind plays an important role in wide estuaries through the generation of relatively strong currents, specifically in shallow areas such as the one object of this study. The wind can generate turbulent mixing that may have an influence in the values of velocity obtained during the monitoring sessions. Wind speed data observed during the two monitoring days was obtained from Weather Underground website (www.wunderground.com) and is shown in Table 4.6.

Table 4.6. Wind Speed - Source: wunderground.com

Date	Wind speed (mph)
July 21 2016 10:00 AM	3.5 calm
July 21 2016 4:00 PM	6.9 E
July 22 2016 10:00 AM	8.1 SW
July 22 2016 4:00 PM	15 SSW

4.3.1.4. Tides

Tidal information is a fundamental mechanism for estuarine mass flux, and an essential element to calculate net estuarine flow, and to analyze the magnitude of the factors dictating dispersion coefficient characteristics such as velocity and salinity concentration gradient. Hours of in-situ monitoring (10:00 AM and 4:00 PM) were selected to coincide the rising and falling phases of the tidal cycle, to capture variations of flow and salinity concentrations over flood and ebb cycles. It was observed that the monitoring dates were influenced by the Spring Tides.

Tidal information collected from NOAA for Station ID 8638379 (referenced to Station ID 8638610 – Sewells Point) for July 21st and July 22nd is shown in Figure 4.5. Tidal variations over the month of July for station are also shown in Figure 4.6.

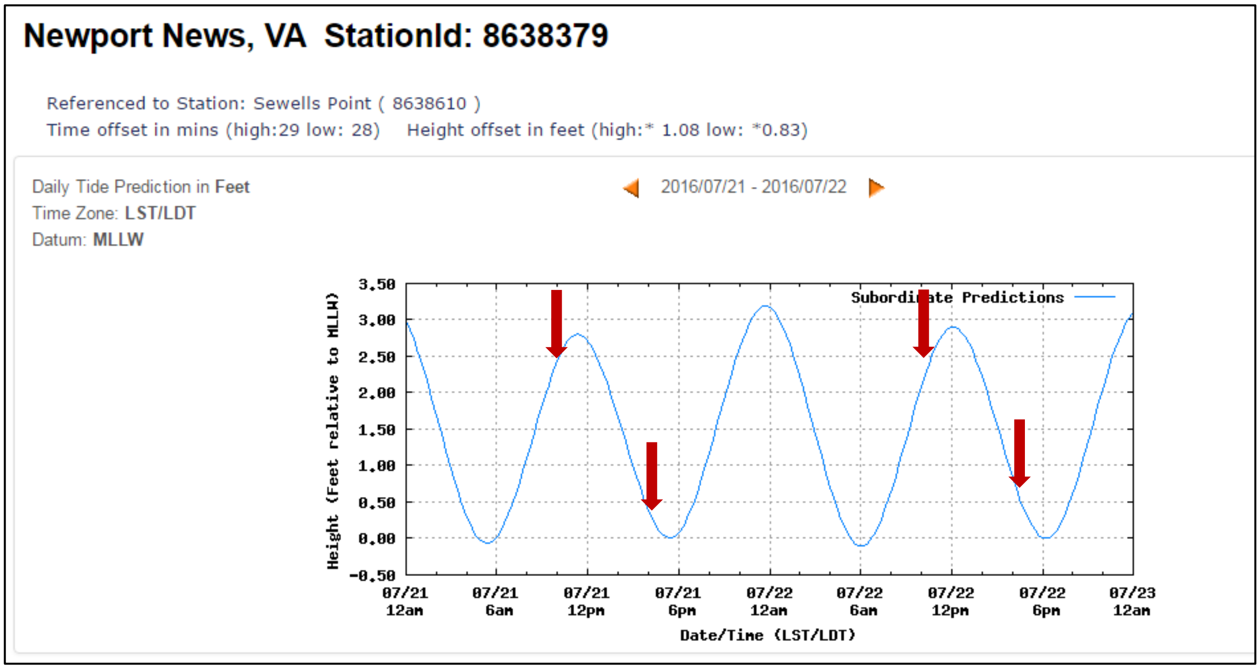

Figure 4.5. Tidal Cycles on July 21st and 22nd

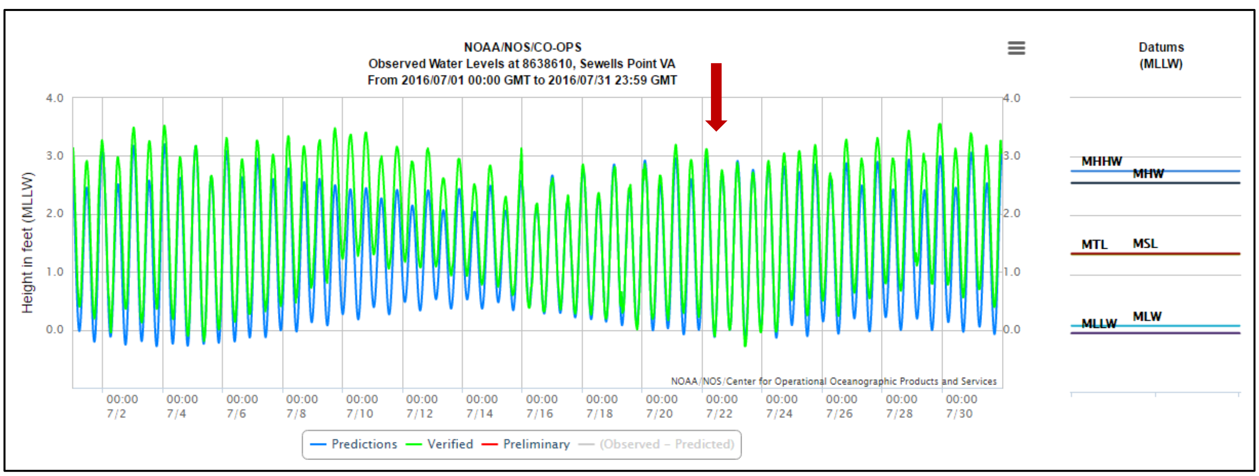

Figure 4.6. Water Levels for the month of July 2016

4.3.2. Dispersion Coefficient

As salinity is considered a “natural” tracer, it was possible to predict the longitudinal dispersion coefficient based on variations in salinity concentration along the area of study, and to apply Eq. (1.5) shown below and estimate its slope which contains the dispersion coefficient, E.

$$ln\frac{S}{S_0} = \frac{U}{E}x$$

where

S = Salinity concentration
S_0 = Source concentration at x = 0
u = Net (tidal-averaged) velocity due to freshwater flow
x = Distance from the mouth to upstream river (negative values)
E = Dispersion coefficient

Estimation of dispersion coefficient was performed by considering following two intertidal calculation approaches:

1. Average of salinity concentrations per segment and per tidal cycle (Ebb and Flood, respectively)
2. Average of all salinity concentrations per segment collected during two consecutive days

Detailed dispersion coefficient calculations for each approach are listed in Appendix I. The estimated error in the determination of dispersion coefficient values is ~ 20% based on the accuracy of the velocity, salinity and distance measurements. The results are summarized in Table 4.7.

Table 4.7. Dispersion coefficient values per segment

Segment	Dispersion Coefficient (m^2/s)		
	Flood Cycle	**Ebb Cycle**	**Averaged Cycles**
1 and 1’	10000	3000	4500
2	-10000	5400	38000
3	2400	3000	2600
4	-34000	7000	11000
5 and 5’	9000	6000	8000
6,7 and 8	46000	3200	5000

4.3.3. Tidal Cycle Flow and Net Estuarine Flow

To determine flow on each segment and between adjacent segments, two approaches are considered for a comparative study.

1. **Tidal Cycle Flow:** Applicable to the characterization of TSS per tidal cycles. Tidal cycle flow is the product of average velocity per segment and segmental cross-sectional area in x- or y-direction where x-direction is along with the shoreline, and y-direction is lateral to the shoreline:

$$Q_{i.j} = A_c U_{i,j} \qquad \text{Eq. (4.10)}$$

where

$Q_{i.j}$ = Flow from segment i to j

A_c = Cross sectional area between segments i and j

$U_{i,j}$ = Average velocity between segments i and j

2. **Net Estuarine Flow**: Used in the characterization of TSS for averaged cycles. Net Estuarine Flow, Q_n, refers to the advective movement of water out of the estuary over a tidal cycle or a given number of tidal cycles (Chapra, 2008):

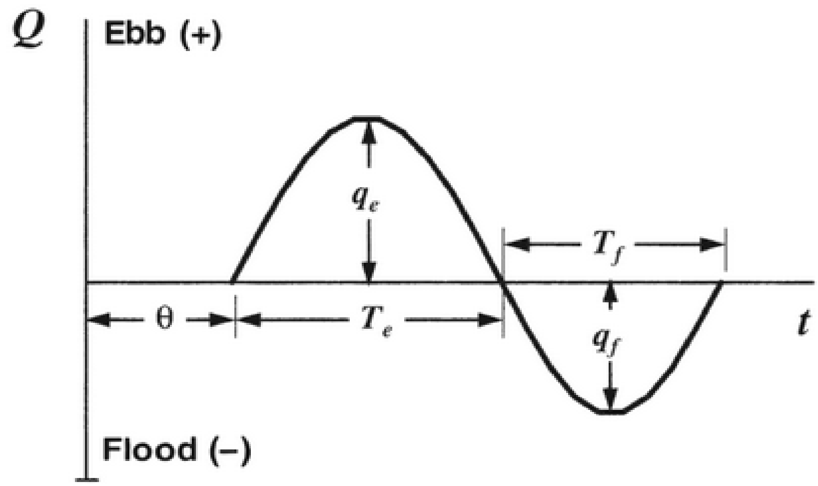

Figure 4.7. Net Estuarine Flow

$$Q_n = \frac{2}{\pi} * \frac{q_e T_e - q_f T_f}{T_e + T_f} \qquad \text{Eq. (4.11)}$$

where

q_e = Flow at ebb cycle

T_e = Ebb cycle duration (25200 seconds)

q_f = Flow at flood cycle

T_f = Flood cycle duration (21600 seconds)

In this approach, q_e and q_f are calculated using the tidal cycle flow, while T_e and T_f are defined from the tidal cycles duration for July 21st and 22nd obtained from NOAA.

At each ebb and flood tidal cycle, flows were calculated with average segmental velocities and cross-sectional areas. The net estuarine flow was then calculated based on the obtained values of ebb and flood flows to subsequently be utilized in the Steady State Response Matrix, whether to determine the advective flow at the interface of the evaluated segments or to determine the internal loading (W) per segment. Results of Tidal Cycle Flow and Net Estuarine Flow are listed in Appendix II.

4.3.4. Bulk Dispersion Coefficient

Bulk dispersion coefficient, E' is a bulk exchange flow going each way between compartments and is not equivalent to measured dispersion coefficients estimated from dye studies. (Schnoor, 1996)

The bulk dispersion coefficient can be estimated from the values of the dispersion coefficient. This estimation requires determining the values of dispersion coefficient at the interface of the segments. One approach to calculate this interface values is to apply the weighted –difference formulation (Chapra, 2008):

$$E_{j,k} = \alpha_{j,k} E_j + \beta_{j,k} E_k \qquad \text{Eq. (4.12)}$$

where

$$\alpha_{j,k} = \frac{\Delta x_k}{\Delta x_j + \Delta x_k} \qquad \text{Eq. (4.13)}$$

$$\beta_{j,k} = \frac{\Delta x_j}{\Delta x_j + \Delta x_k} \qquad \text{Eq. (4.14)}$$

E_j = Dispersion coefficient of segment j

E_k= Dispersion coefficient of segment k

Δx_k = Length of Segment k

Δx_j = Length of segment j

Once the values of dispersion coefficient at the interfaces are calculated, the bulk dispersion coefficient, E' can be calculated by proportionalizing segmental dimension to the dispersion coefficient with interfacing cross-sectional area and centroidal distance as shown in Eq. (4.15):

$$E'_{j,k} = \frac{E_{j,k} A_c}{\Delta_x} \qquad \text{Eq. (4.15)}$$

where

$E_{j,k}$ = Dispersion coefficient of Interface j,k

A_c = Cross Sectional Area of the interface

Δ_x = Distance between segments – from centroid

Calculated values of dispersion coefficient and bulk dispersion per interface were determined using an estimated error of ~ 20% based on the accuracy of the velocity, salinity and distance measurements. Results are listed in Appendix II and summarized in Table 4.8.:

Table 4.8. Dispersion and Bulk Dispersion Coefficient Values per Interface

Interface	**Flood**		**Ebb**		**Averaged**	
	E (m^2/s)	**E' (m^3/s)**	**E (m^2/s)**	**E' (m^3/s)**	**E (m^3/s)**	**E' (m^2/s)**
5,4	22000	8000	6000	2400	10000	3600
4,3	18000	7200	4900	2000	7000	2700
3,2	6000	25000	4200	1700	21000	8000
2,1	10000	3800	4200	1700	22000	9000
8,7	46000	18000	3200	1300	5000	2200
7,6	46000	19000	3200	1300	5000	2200
8,4	42000	42000	4400	4400	7000	7000
7,3	31000	32000	3100	3200	4500	4500
6,2	34000	33000	3900	3800	16000	16000

4.3.5. Settling

Settling losses can be formulated as a flux of mass across the surface area of the sediment-water interface. Thus, by multiplying the flux by area, settling can be developed as:

$$Settling = K_s VC \qquad \text{Eq. (4.16)}$$

where

K_s = First Order settling rate constant (v/h)

v = Settling Velocity

h = Mean depth of segment

V = Segment Volume

C = Concentration of TSS at segment

The settling velocity is the most fundamental property governing the motion of the sediment particles in water. In Stoke's Law equation, this velocity depends principally on the size, shape and density of the particle and the viscosity and density of the water. Stoke's Law represents the key processes associated to particle settling under a controlled setting, it is not practical to apply to uncontrolled, ambient waterbodies. As a result, many empirical formulas were proposed for estimating the settling velocities, especially for cohesive sediments in ambient, natural waterbodies (Zhen-Gang Ji, 2008).

In this study, an empirical settling velocity, W_s, equation developed in studies using mud from the Severn estuary in the United Kingdom (Zhen-Gang Ji, 2008) was used to reflect cohesive sediments in the study site that are primarily composed by clay, silt and organic matter -- adsorbents of contaminants in water:

$$W_s = 0.513S^{1.29} \quad \text{Eq. (4.17)}$$

where W_s is settling velocity in mm/s and S is the concentration of sediments, and Eq. (4.17) is applicable for $S < 2$ g/L

The concentrations of sediments are estimated using the concentration of Total Suspended Solids of each segment. The values of TSS were estimated by applying study site-specific General Linear Model described in 4.1.1.

Calculated settling velocity (W_s) and the 1st-order Settling constant (K_s) per segment were determined using an estimated error of ~ 2% based on the accuracy of the turbidity and average depth measurements. Results are summarized in Tables 4.9, 4.10 and 4.11

Table 4.9. Settling velocity and first order settling constant at Flood Cycle

Segment	Turbidity (NTU)	TSS Estimation (mg/L)	Settling velocity (m/d)	Average depth (m)	Ks (1/s)
1’		11	0.44	0.9	5.7E-06
8	10.34	17.73	0.82	0.9	1.05E-05
7	9.59	16.45	0.74	0.9	9.5E-06
6	11.53	19.77	0.94	0.9	1.21E-05
5’		11	0.44	0.9	5.7E-06
5	11.39	19.53	0.92	0.45	2.37E-05
4	9.43	16.17	0.72	0.45	1.85E-05
3	15.65	26.84	1.39	0.45	3.58E-05
2	15.35	26.32	1.36	0.45	3.50E-05
1	16.41	28.14	1.48	0.45	3.81E-05

Table 4.10. Settling velocity and first order settling constant at Ebb Cycle

Segment	Turbidity (NTU)	TSS Estimation (mg/L)	Settling Velocity (m/d)	Average Depth (m)	Ks (1/s)
1’		11	0.44	0.9	5.7E-06
8	8.33	14.28	0.62	0.9	8.0E-06
7	9.18	15.74	0.7	0.9	9.0E-06
6	8.87	15.21	0.67	0.9	8.6E-06
5’		11	0.44	0.9	5.7E-06
5	11.65	19.98	0.95	0.45	2.44E-05
4	10.75	18.43	0.86	0.45	2.21E-05
3	10.21	17.51	0.8	0.45	2.06E-05
2	17.11	29.34	1.56	0.45	4.01E-05
1	7.83	13.43	0.57	0.45	1.47E-05

Table 4.11. Settling velocity and first order settling constant at averaged Cycles

Location	**Turbidity (NTU)**	**TSS Estimation (mg/L)**	**Settling velocity (m/d)**	**Average depth (m)**	**Ks (1/s)**
1’		11	0.44	0.9	5.7E-06
8	9.33	16	0.71	0.9	9.1E-06
7	9.38	16.09	0.72	0.9	9.3E-06
6	10.2	17.49	0.8	0.9	1.03E-05
5’		11	0.44	0.9	5.7E-06
5	11.52	19.76	0.94	0.45	2.42E-05
4	10.09	17.3	0.79	0.45	2.03E-05
3	12.93	22.17	1.09	0.45	2.80E-05
2	16.23	27.83	1.46	0.45	3.76E-05
1	12.12	20.78	1	0.45	2.57E-05

Note: TSS values for boundaries 1’ and 5’ were estimated from Station LE.5 (Source: VECOS-VIMS)

4.3.6 Internal Loading (W)

Main objective of this study is to characterize the concentration of Total Suspended Solids in the study area by evaluating the interaction between advective and dispersive processes within control volume segments, and subsequently, to assess their influence in the final TSS concentration per segment at steady state condition. Therefore, it is necessary to first estimate the internal loading, or concentration of Total Suspended Solids on each of the evaluated segments to establish a baseline.

The internal loading was calculated using the concentration of Total Suspended Solids times the Flow per segment and the values were determined using an estimated error of ~ 2% based on the accuracy of the turbidity and velocity measurements. The results are shown in Table 4.12.

Table 4.12. Internal Loading Per Segment

Segment	Flood Cycle			Ebb Cycle			Averaged Cycles		
	TSS estimate (mg/L)	**Q (m^3/s)**	**W (g/s)**	**TSS estimate (mg/L)**	**Q (m^3/s)**	**W (g/s)**	**TSS estimate (mg/L)**	**Qn (m^3/s)**	**W (g/s)**
1’	11	19.78	218	11	24.93	274	11	2.73	30
8	17.73	15.83	281	14.28	16.71	239	16	1.08	173
7	16.45	23.64	389	15.74	42.02	660	16.09	7.46	120
6	19.77	20.7	409	15.21	26.1	397	17.49	2.86	50
5’	11	15.01	165	11	15.84	174	11	1.02	11.2
5	19.53	15.01	293	19.98	25.01	500	19.76	4.16	82
4	16.17	14.95	242	18.43	23.75	438	17.3	3.75	65
3	26.84	14.88	399	17.51	15.76	276	22.17	1.03	22.8
2	26.32	17.1	450	29.34	24.3	710	27.83	3.31	92
1	28.14	16.34	460	13.43	15.48	208	20.78	0.51	10.6

Note: TSS values for boundaries 1’ and 5’ were estimated from Station LE.5 (Source: VECOS-VIMS)

4.3.7. TSS Characterization

To find the concentration of Total Suspended Solids per segment influenced by resultant flux from the interaction of advective and dispersive processes among adjacent segments, Steady State Response Matrix (SSRM) method was used.

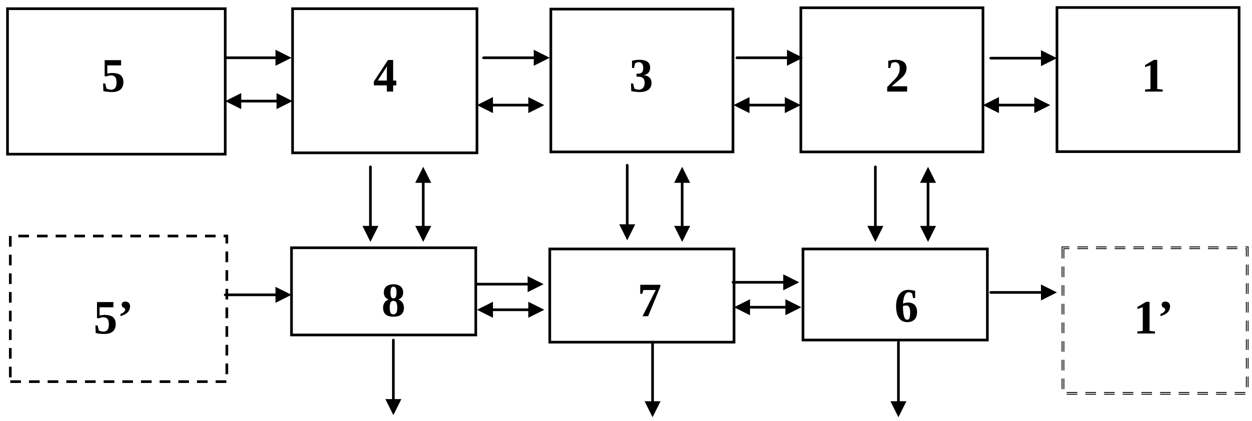

Figure 4.8. Segments diagram

Segments 1, 1’, 5 and 5’ were used as boundary conditions and therefore no mass balance equations were developed.

Resultant finite segment matrix includes a series of six equations with six unknown concentrations:

Seg. 2: $C_2\left(Q_{2,1}+Q_{2,6}+E'_{3,2}+E'_{2,1}+E'_{2,6}+K_{S2}V_2\right)-C_3\left(Q_{3,2}+E'_{3,2}\right)-C_6E'_{2,6}=W_2+C_1E'_{2,1}$

Seg. 3: $-C_2E'_{3,2}+C_3\left(Q_{3,2}+Q_{3,7}+E'_{4,3}+E'_{3,2}+E'_{3,7}+K_{S3}V_3\right)-C_4\left(Q_{4,3}+E'_{4,3}\right)-C_7E'_{3,7}=W_3$

Seg. 4: $-C_3E'_{4,3}+C_4\left(Q_{4,3}+Q_{4,8}+E'_{5,4}+E'_{4,3}+E'_{4,8}+K_{S4}V_4\right)-C_8E'_{4,8}=W_4+C_5\left(Q_{5,4}+E'_{5,4}\right)$

Seg. 6: $C_2\left(Q_{2,6}+E'_{2,6}\right)-C_6(Q_{6,1'}+Q_{6Y}+E'_{7,6}+E'_{2,6}+K_{S6}V_6)+C_7\left(Q_{7,6}+E'_{7,6}\right)=W_6$

Seg. 7: $-C_3\left(Q_{3,7}+E'_{3,7}\right)-C_6E'_{7,6}+C_7\left(-Q_{7Y}+Q_{7,6}+E'_{8,7}+E'_{3,7}+E'_{7,6}+K_{S7}V_7\right)-C_8(Q_{8,7}+E'_{8,7})=W_7$

Seg. 8: $-C_4\left(Q_{4,8}+E'_{4,8}\right)-C_7E'_{8,7}+C_8\left(-Q_{8Y}+Q_{8,7}+E'_{4,8}+E'_{8,7}+K_{S8}V_8\right)=W_8-C_{5'}Q_{5',8}$

Collecting terms for C_i, TSS concentrations:

a = $\left(Q_{2,1}+Q_{2,6}+E'_{3,2}+E'_{2,1}+E'_{2,6}+K_{S2}V_2\right)$

b = $\left(Q_{3,2}+E'_{3,2}\right)$

c = $W_2+C_1E'_{2,1}$

d = $\left(Q_{3,2}+Q_{3,7}+E'_{4,3}+E'_{3,2}+E'_{3,7}+K_{S3}V_3\right)$

e = $\left(Q_{4,3} + E'_{4,3}\right)$

f = $\left(Q_{4,3} + Q_{4,8} + E'_{5,4} + E'_{4,3} + E'_{4,8} + K_{S4}V_4\right)$

g = $W_4 + C_5\left(Q_{5,4} + E'_{5,4}\right)$

h = $\left(Q_{2,6} + E'_{2,6}\right)$

i = $(Q_{6,1'} + Q_{6Y} + E'_{7,6} + E'_{2,6} + K_{S6}V_6)$

j = $\left(Q_{7,6} + E'_{7,6}\right)$

k = $\left(Q_{3,7} + E'_{3,7}\right)$

l = $\left(-Q_{7Y} + Q_{7,6} + E'_{8,7} + E'_{3,7} + E'_{7,6} + K_{S7}V_7\right)$

m = $(Q_{8,7} + E'_{8,7})$

n = $\left(Q_{4,8} + E'_{4,8}\right)$

o = $\left(-Q_{8Y} + Q_{8,7} + E'_{4,8} + E'_{8,7} + K_{S8}V_8\right)$

p = $W_8 - C_{5'}Q_{5',8}$

Then the Steady State Response Matrix can be developed as:

$$\begin{bmatrix} a & -b & 0 & -E'_{2,6} & 0 & 0 \\ -E'_{3,2} & d & -e & 0 & -E'_{3,7} & 0 \\ 0 & -E'_{4,3} & f & 0 & 0 & -E'_{4,8} \\ h & 0 & 0 & -i & j & 0 \\ 0 & -k & 0 & -E'_{7,6} & l & -m \\ 0 & 0 & -n & 0 & -E'_{8,7} & o \end{bmatrix} \begin{Bmatrix} C_2 \\ C_3 \\ C_4 \\ C_6 \\ C_7 \\ C_8 \end{Bmatrix} = \begin{Bmatrix} c \\ W_3 \\ g \\ W_6 \\ W_7 \\ p \end{Bmatrix}$$

Substituting values for three scenarios – Flood cycle averaged, Ebb cycle averaged, and Averaged cycles --, estimated Total Suspended Solids per segment influenced by resultant flux from the interaction of advective and dispersive processes among adjacent segments are summarized in Table 4.13.

Table 4.13. TSS concentration per segment

Segment	TSS concentration at Flood Cycle (mg/L)	TSS Concentration on Ebb Cycle (mg/L)	TSS concentration at averaged cycles (mg/L)
2	23.75	16.36	25.48
3	22.55	18.13	28.21
4	21.73	19.16	25.74
6	23.34	16.85	26.62
7	22.66	18.64	34.80
8	22.03	19.20	27.82

CHAPTER 5.

ANALYSIS OF RESULTS AND CONCLUSIONS

Estimation of site-specific longitudinal dispersion coefficient using variation in salinity concentrations was performed in a small study area of the tidal section of the James River in Newport News, Virginia. The procedure considered the variation in salinity concentrations per tidal cycle and per averaged tidal cycles with the purpose to estimate longitudinal and lateral dispersion coefficients along the shoreline, then further characterize estuarine mixing and transport mechanisms of Total Suspended Solids in the study area.

Salinity and turbidity values collected during the two days of monitoring did not show significant variations in the transversal dimension, contrasting with the notorious changes in velocity measurements, which directly influence the values of Dispersion Coefficient. This site-specific condition motivated the application of a two-dimensional model where only the vertical variation of salinity and velocity were considered negligible, allowing this shallow portion of the James River to be treated as a homogenous profile and a reasonable and simplistic evaluation of the characteristics of TSS transport in the evaluated segments.

Velocity is a significant influencing component in the evaluation of TSS transport mechanisms due to its direct impact on the estimation of the dispersion coefficient. In shallow and open areas of the estuary, wind is the most influencing factor contributing to the velocity variation. Variation in freshwater discharge is generally insignificant in comparison to the tidal velocity. During the days of the monitoring, the presence of relatively mild winds appeared to have little influence on the velocity values obtained. In contrast, the strong spring tidal force present during these days, seemed to have a direct influence in the relatively high values of tidal velocity and subsequent high values of estimated dispersion coefficient.

Although dispersion coefficients of large magnitudes are expected in a wider river like the James River with strong influence of salinity intrusion and limited shear flow, estimated dispersion coefficients show a broad range (2572 m^2/s through 46000 m^2/s) of variations, and indicate evidence of its estuarine complexity where river flow, tidal range and sediment distribution are constantly changing due to the influence of weather conditions. This is particularly clear in the observed negative values of dispersion coefficient during the flood cycle, where there is a strong influence of salinity intrusion towards the upstream part of the study area.

Initial objective of this study was to evaluate mixing and transport of Total Suspended Solids in the study area receiving nearby effluent discharge from the HRSD James River Wastewater Treatment Plant. However, in-situ sampling of TSS concentrations in the study were approximately 10 to 20 times higher than the actual concentration of TSS in the effluent discharge. This suggests that the actual TSS discharge of the plant will have a minimum or a null effect toward the concentration of TSS along the area of study. The seek approach of this study was then, to apply the Steady State Response Matrix (SSRM) method and evaluate the characteristics of TSS transport on three scenarios: Flood cycle averaged, Ebb cycle averaged, and Averaged cycles with the purpose of analyze resultant TSS concentration estimates with respect to in-situ measured TSS concentrations.

The obtained results are summarized in the following Figures 5.1. through 5.3.

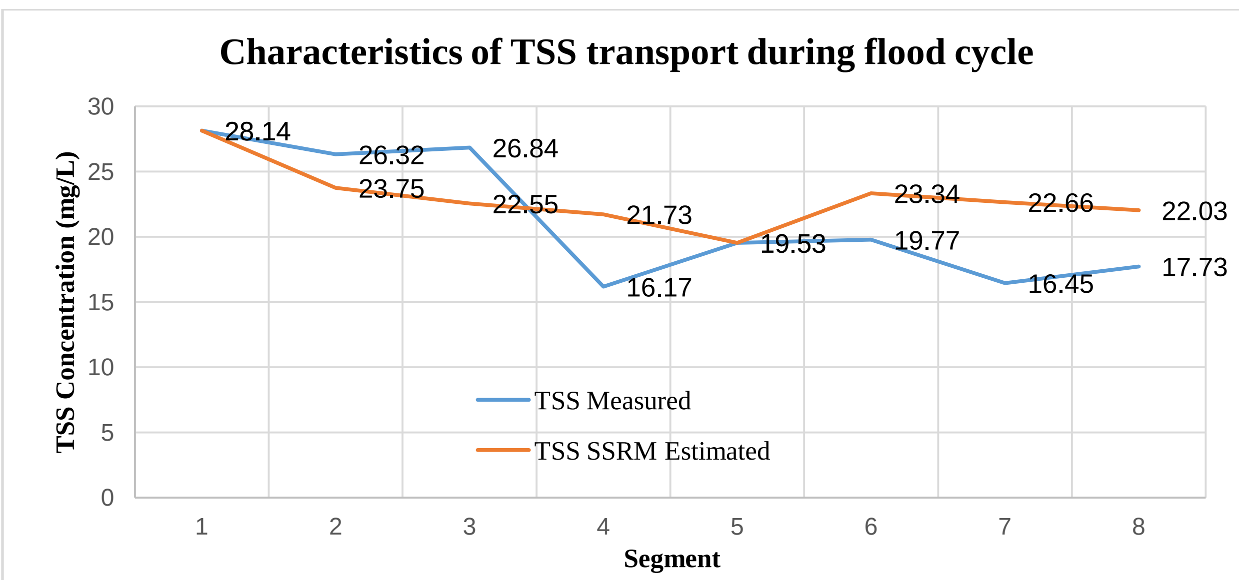

Figure 5.1. Characteristics of TSS transport during flood cycle

During flood cycle, Finite Segment Method estimate results showed that segments 4, 6, 7 and 8 were significantly influenced by dispersive mixing and advective transport of TSS from segments 2 and 3, which is expected considering that during flood cycle water moves from downstream of the estuary towards the upstream.

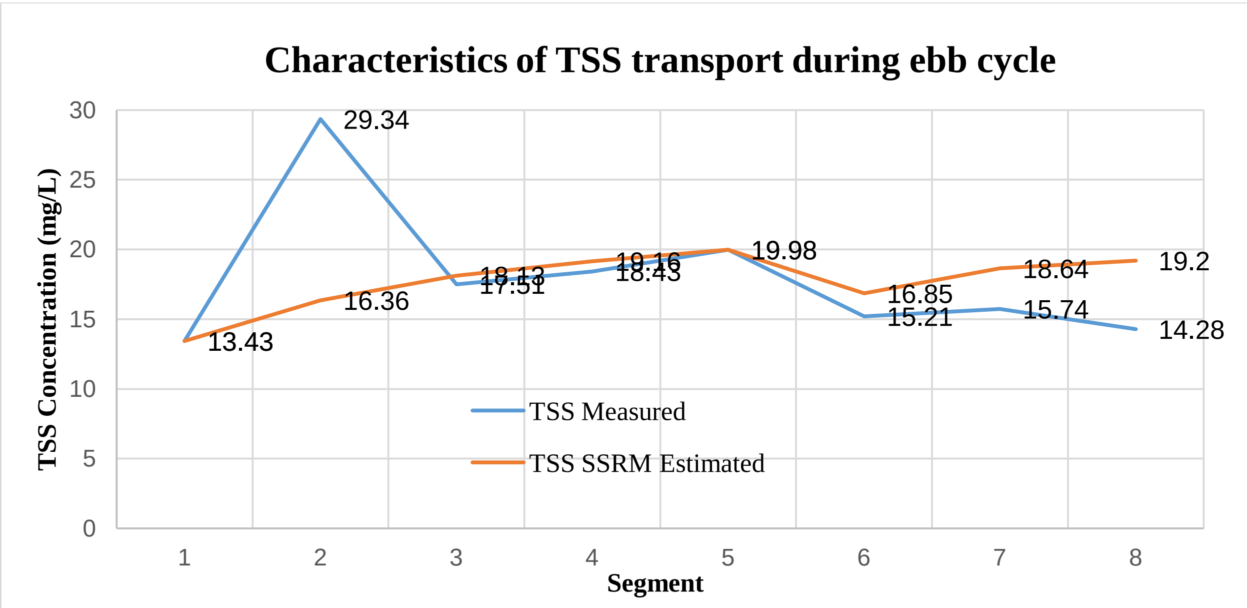

Figure 5.2. Characteristics of TSS transport during ebb cycle

During ebb cycle, Finite Segment Method estimate results showed that only segment 2 experienced a significant drop in concentration, most likely, indicative of advective transport movement of TSS from segment 2 towards segments 1 and 6, with the latest showing a slightly increase on TSS concentration. Changes in concentrations for Segments 3 and 4 were almost negligible, which is expected due the similarity in TSS concentrations among these two segments and segment 5.

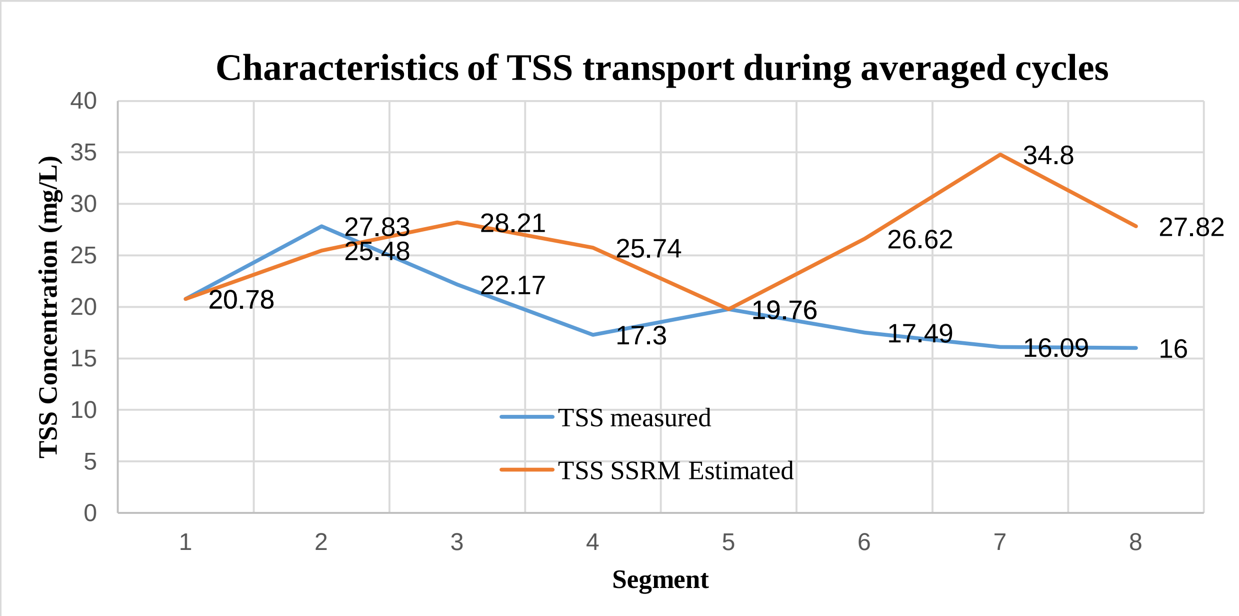

Figure 5.3. Characteristics of TSS transport during averaged cycles

The Finite Segment Method estimate results for the averaged cycles evidence a high increase in concentrations of TSS for almost all segment evaluated, with the highest values on segments 6, 7 and 8. These results suggest that dispersive transport is dominant over advective transport in this particular area of the James River.

The dispersive transport dominance was clearly evidenced with the high values of dispersion coefficient obtained for all three scenarios evaluated and it was further revealed with the estimated changes in concentration of TSS using the Finite Segment Method. For this particular area of study, tides exercise great influence over mixing and transport of substances more than the low volume of freshwater inflow coming from the Warwick River.

One of the major assumptions of this study was to consider a steady state condition in order to apply the Finite Segment Method. This method allowed the simulation of TSS concentration in the area of study in a simplified manner through its segmentation and the evaluation of parameters collected during one tidal cycle per day for two consecutive days. This was particularly facilitated and feasible in the particular studied area, where the James River is wide and shallow, and the section of the river studied encompasses a small area.

It is important to recognize, however, that due to the constant variation of the estuary parameters influenced by atmospheric conditions that affect the dispersion coefficient and concentration of TSS, such as the velocity variations during spring and neap tides, it is recommended to include a wider range of weather conditions and apply a statistical approach such as a minimum of 10 days in order to obtain and estimate of the mean flow unaffected by wind (Dyer, 1997). In similar manner, where estuary hydrodynamics are more complex, some authors recommend the application of monitoring procedures that involve repetitive sampling of three times on each tidal cycle at (1) high tide, (2), mean tide (half interval between high and low tide), and (3) low tide; repeated daily over 28-day period at a proper sample depth of about ¼ to 1/3 distance to the bottom in order to capture variations and influence of spring and neap tides.

The methodology applied to this study was used to establish Total Suspended Solids concentrations characteristic over time and distance in a small tidal section of the James River. The incorporation of the Finite Segment Method and the Steady State Response Matrix allowed the evaluation of the mechanisms of TSS transport as well as the analysis of influencing parameters such as Dispersion coefficient, Total Suspended Solids concentration and advective/dispersive flow dominance for this site-specific location.

Finally, the site-specific General Linear Model (GLM) model, developed and utilized to obviate the time consuming method required for determining Total Suspended Solids concentrations, was successfully applied to sampled values of Turbidity obtained during this study for values of TSS between1.5 and 27.5 mg/L. Estimated Total Suspended Solids data was subsequently and successfully used in Finite Segment Method (FSM) and the Steady State Response Matrix (SSRM) to characterize the Total Suspended Solids mixing and transport in the study area.

For values of TSS estimated well above 27.5 mg/l, such as the ones obtained in the SSRM for the averaged cycles on segment 7 and the ones estimated from in situ measurements of segment 2 at ebb cycle, it is possible that a different TSS/Turbidity relationship will apply.

REFERENCES

Al Yaseri, Isam; Morgan, Susan and Retzlaff, William (2013). *Using Turbidity to Determine Total Suspended Solids in Storm-Water Runoff from Green Roofs*. Journal of Environmental Engineering. 139(6): 822-828.

Chapra, Steven (2008), Surface Water Quality Modeling, Waveland Press, Inc., Long Grove, IL, ISBN 1-57766-605-4

Dyer, Keith (1997), Estuaries A Physical Introduction, Wiley, Chichester, England, ISBN 0-471-97470-4

Eagleson, Peter S., Ippen, Arthur T. (1966), Estuary and Coastline Hydrodynamics, McGraw Hill. Massachusetts Institute of Technology. Hydrodynamics Laboratory, ISBN 0-070320154

Fischer, Hugo B. (1968), Methods for Predicting Dispersion Coefficients in Natural Streams, with Application to Lower Reaches of the Green and Duwamish Rivers Washington. United States Department of Interior. Geological Survey Professional Paper 582-A. 34 p.

Fischer, Hugo B. et al (1979), Mixing in Inland and Coastal Waters, Academic Press, New York, New York, ISBN 0-12-258150-4

James, A. (1993), An Introduction to Water Quality Modeling, Wiley, West Sussex, England, ISBN 0-471-92347-8

Line, D.E.; Hall, K.R. and Blackwell, J.D. (2013). *Estimating Suspended Solids from Turbidity in the Robeson Creek, NC Watershed*. Journal of the American Water Resources Association. 49(6):1412-1420.

Martin, James L., McCutcheon, Steve C. (1999), Hydrodynamics and Transport for water Quality Modeling, Lewis, Boca Raton, Florida, ISBN 0-87371-612-4

Martin, James L., (2007), *Linear Superposition in Total Maximum Daily Loads Applications: The Steady-State Response Matrix Revisited.* Journal of the American Water Resources Association (JAWRA), 43(5): 1270-1279.

Miller, E.G., (1960), An Introduction to the Calculus of Finite Differences and Difference Equations, Henry Holt, New York.

Montgomery, Douglas; Runger, George (2014), *Applied Statistics and Probability for Engineers.* Wiley, Danvers, Massachusetts, ISBN 13 9781118539712.

Nemerow, Nelson L. (1985), Stream, Lake, Estuary and Ocean Pollution, Van Nostrand Reinhold Company, New York, ISBN 0-442-26720-7

NOAA Tides and Currents - https://tidesandcurrents.noaa.gov/

Rinaldi, S. Soncini-Sessa, R., Stehfest, H. and Tamura, H. (1979), Modeling and Control of River Quality, Mc Graw Hill, Great Britain, ISBN0-07-052925-6

Rügner, Hermann et al (2013). *Turbidity as Proxy for Total Suspended Solids (TSS) and Particle Facilitated Pollutant Transport in Catchment*. Water and Air System Science.69:373-380.

Schnoor, Jerald L. (1996), *Environmental Modeling*, Wiley, New York, New York, ISBN 0-471-12436-2

Shana, D.C., Cho, Y.-K, Kwak, M.-T., Kundu, S.R and Jung, K.T. (2011), *Spatial variation of the longitudinal dispersion coefficient in an estuary.* Hydrology and Earth System Science, 15: 3679-3688

Thomann, R.V., (1983). Finite Difference Approach to Estuary Water Quality Analysis, in Quality Models of Natural Water Systems, Twenty-Eight Summer Institute in Water Pollution Control, Manhattan College.

Thomann, R., & Muller, J.A. (1987). Principles of Surface Water Quality Model and Control. Harper & Row, New York, NY, ISBN 0-060-46677-4

Virginia Department of Environmental Quality (2007). *Fecal Bacteria Total Maximum Daily Load Development for Warwick River – Primary Contact Recreational Use and Shellfish Harvesting.*

Virginia Institute of Marine Science – Virginia Estuarine and Coastal Observing System - http://web2.vims.edu/vecos/

Wilber, Anne Catherine (1986). *Formation of Longitudinal Dispersion Coefficient in Partially Mixed Estuaries and Application in a One-Dimensional Real-time Model*. Dissertation. Virginia Institute of Marine Science, College of William and Mary in Virginia.

Zhen-Gang, Ji (2008), Hydrodynamics and Water Quality, Wiley, Hoboken, NJ, ISBN 978-0-470-13543-3

APPENDIX I.
DISPERSION COEFFICIENT CALCULATIONS PER SEGMENT

A1.1. Per Tidal Cycle – Ebb Cycle

Location	Distance (m)	Salinity (ppt)	U (m/s)
5b	-1108	7.57	
5	-992.5	7.64	0.3
4b/5a	-877	7.66	
4	-767.5	7.68	0.27
3b/4a	-658	7.73	
3	-548	7.83	0.18
2b/3a	-438	7.84	
2	-331	7.94	0.27
1b/2a	-224	7.92	
1	-112	7.96	0.18
1a	0	8.02	

Location	Distance (m)	Salinity (ppt)	U (m/s)
8	-436.5	7.68	0.19
7	-217	7.88	0.48
6	0	8.04	0.29

Location	Distance (m)	Salinity (ppt)	ln (S/So)	U (m/s)
5b	-231	7.57	-0.011818916	
5	-115.5	7.64	-0.002614381	0.3
5a/4b	0	7.66	0	
			Average U	**0.3**

E = 6000 m^2/s

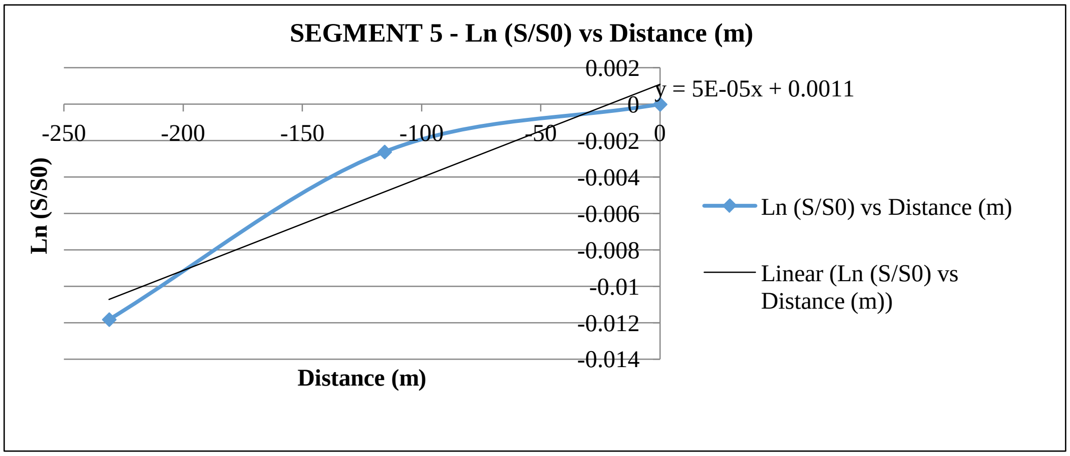

Location	Distance (m)	Salinity (ppt)	ln (S/So)	U (m/s)
4b/5a	-219	7.66	-0.009096879	
4	-109.5	7.68	-0.006489315	0.27
4a/3b	0	7.73	0	
			Average U	**0.27**

E = 6750 m^2/s

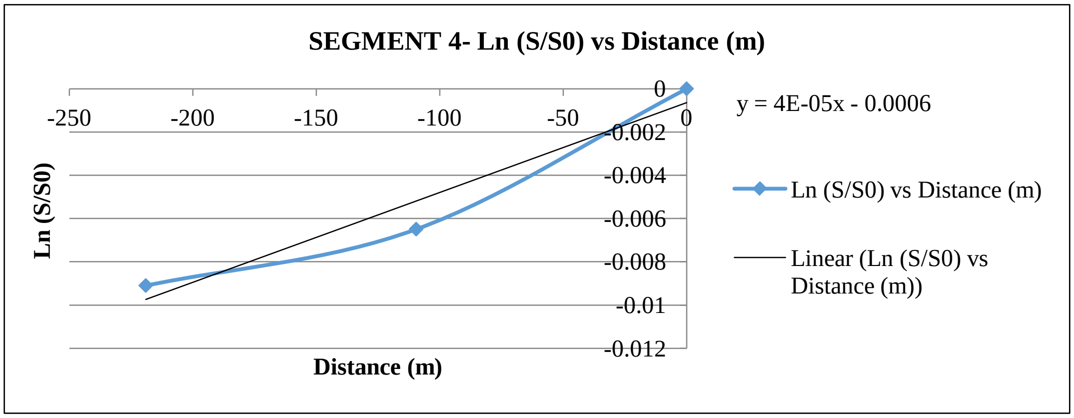

Location	Distance (m)	Salinity (ppt)	ln (S/So)	U (m/s)
3b/4a	-220	7.73	-0.014129972	
3	-110	7.83	-0.001276324	0.18
3a/2b	0	7.84	0	
			Average U	**0.18**

E = 3000 m^2/s

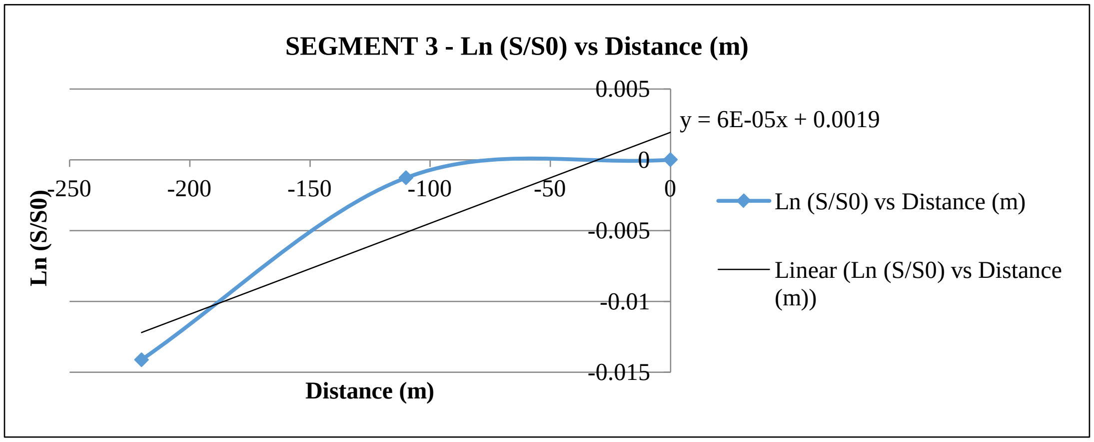

Location	Distance (m)	Salinity (ppt)	ln (S/So)	U (m/s)
2b/3a	-214	7.84	-0.010152371	
2	-107	7.94	0.002522069	0.27
2a/1b	0	7.92	0	
			Average U	**0.27**

E = 5400 m^2/s

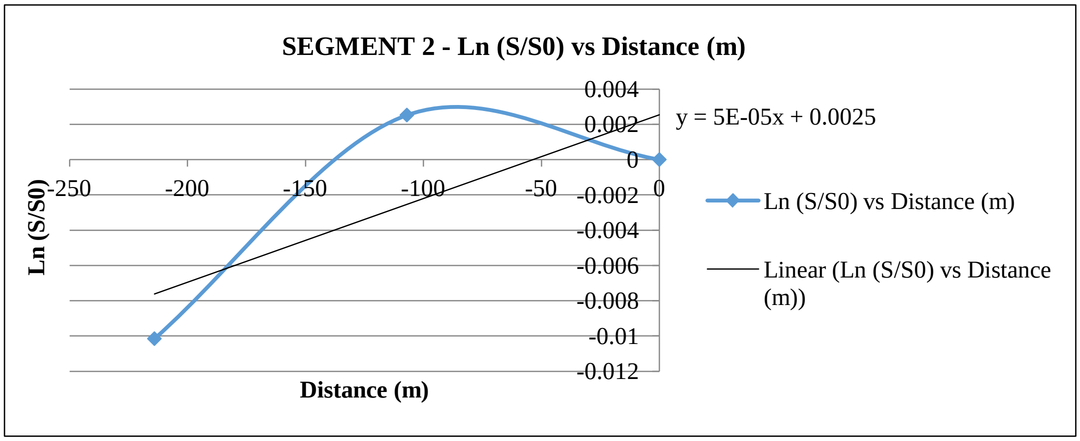

Location	Distance (m)	Salinity (ppt)	ln (S/So)	U (m/s)
1b/2a	-224	7.92	-0.012547216	
1	-112	7.96	-0.007509422	0.18
1a	0	8.02	0	
			Average U	**0.18**

E = 3000 m^2/s

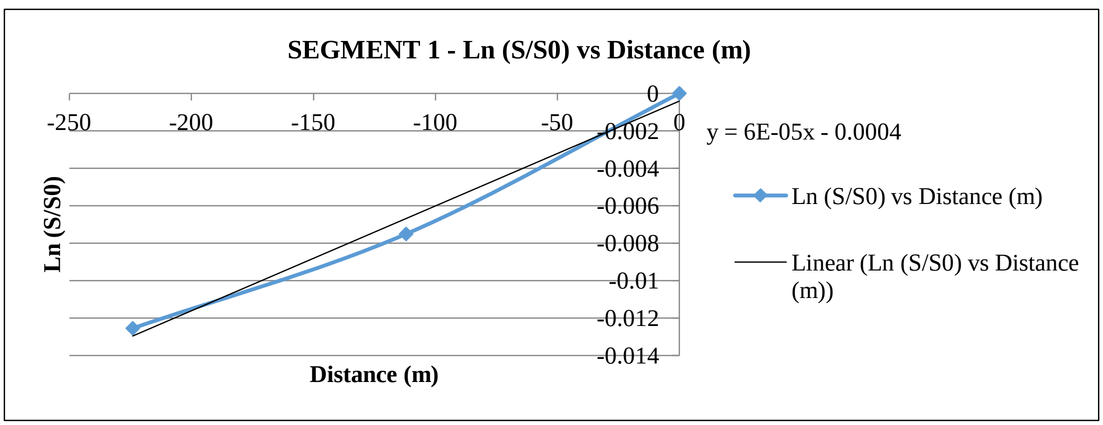

Location	Distance (m)	Salinity (ppt)	ln (S/So)	U (m/s)
8	-436.5	7.68	-0.045809536	0.19
7	-217	7.88	-0.020101179	0.48
6	0	8.04	0	0.29
			Average U	**0.32**

E = 3200 m^2/s

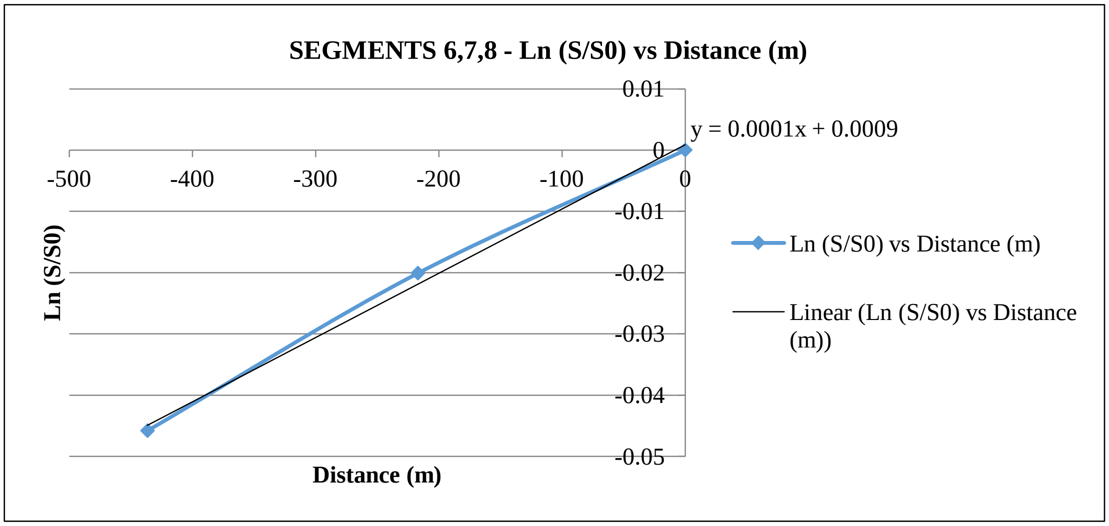

A1.2. Per Tidal Cycle – Flood Cycle

Location	Distance (m)	Salinity (ppt)	U (m/s)
5b	-1108	8.86	
5	-992.5	8.87	0.18
4b/5a	-877	8.9	
4	-767.5	8.89	0.17
3b/4a	-658	8.89	
3	-548	8.94	0.17
2b/3a	-438	9.03	
2	-331	8.99	0.19
1b/2a	-224	8.99	
1	-112	8.91	0.19
1a	0	9.04	

Location	Distance (m)	Salinity (ppt)	U (m/s)
8	-436.5	8.99	0.18
7	-217	8.97	0.27
6	0	9.01	0.23

Location	Distance (m)	Salinity (ppt)	ln (S/So)	U (m/s)
5b	-231	8.86	-0.004504512	
5	-115.5	8.87	-0.00337648	0.18
5a/4b	0	8.9	0	
			Average U	**0.18**

E = 9000 m^2/s

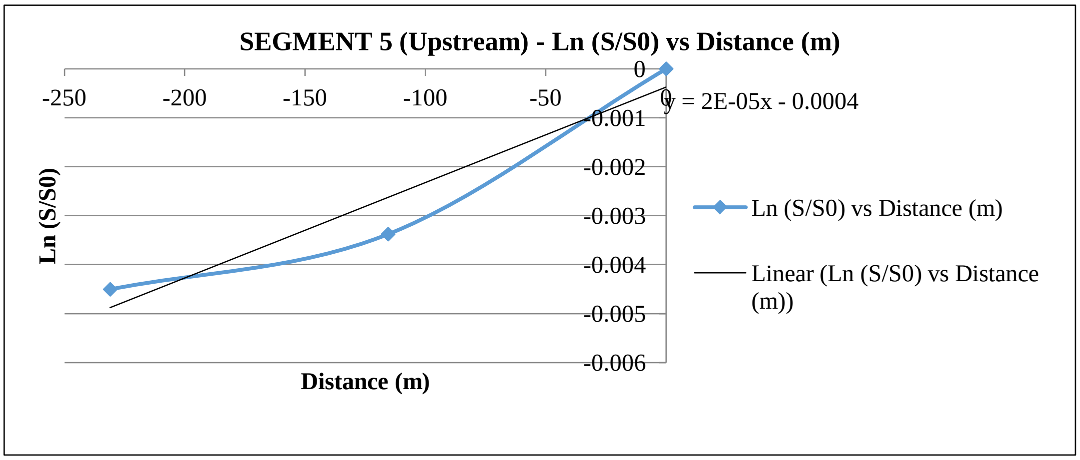

Location	Distance (m)	Salinity (ppt)	ln (S/So)	U (m/s)
4b/5a	-219	8.9	0.001124227	
4	-109.5	8.89	0	0.17
4a/3b	0	8.89	0	
			Average U	**0.17**

E = -34000 m^2/s

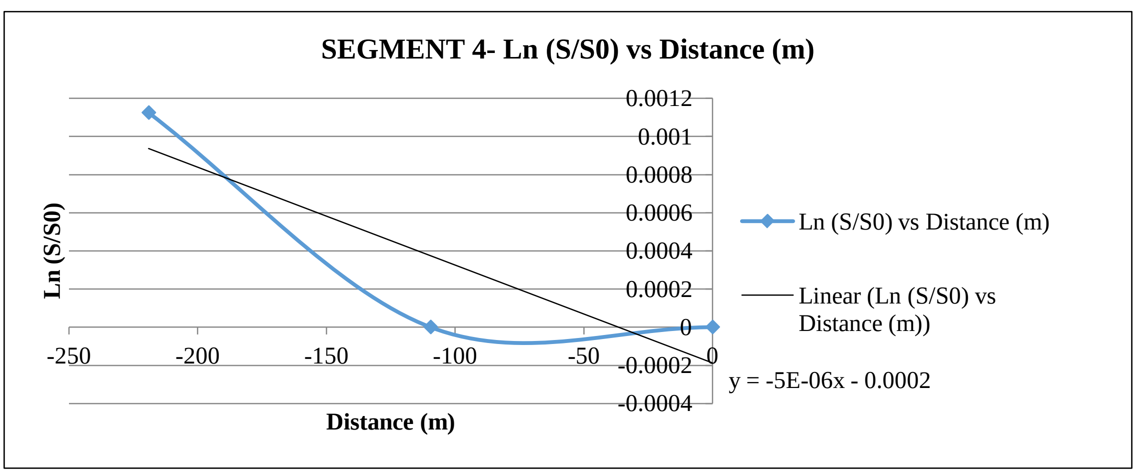

Location	Distance (m)	Salinity (ppt)	ln (S/So)	U (m/s)
3b/4a	-220	8.89	-0.015625318	
3	-110	8.94	-0.010016778	0.17
3a/2b	0	9.03	0	
			Average U	**0.17**

E = 2429 m^2/s

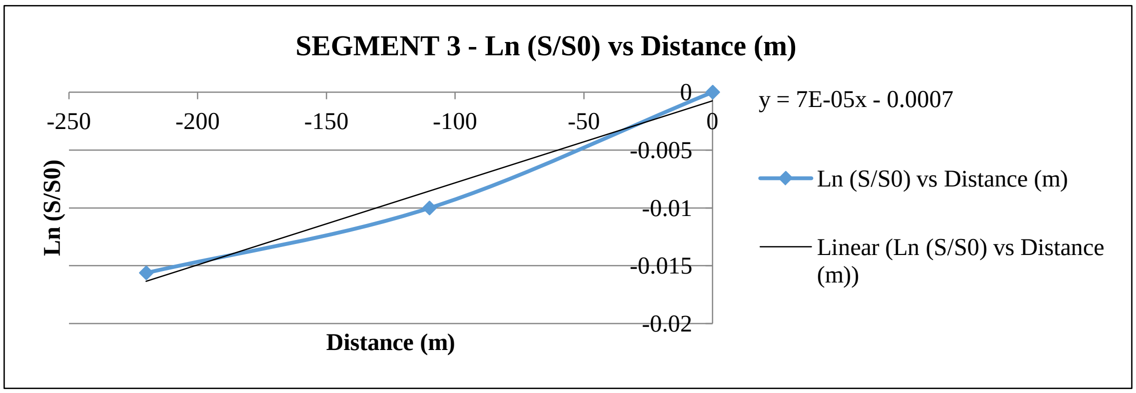

Location	Distance (m)	Salinity (ppt)	ln (S/So)	U (m/s)
2b/3a	-214	9.03	0.004439519	
2	-107	8.99	0	0.19
2a/1b	0	8.99	0	
			Average U	**0.19**

E = -9500 m^2/s

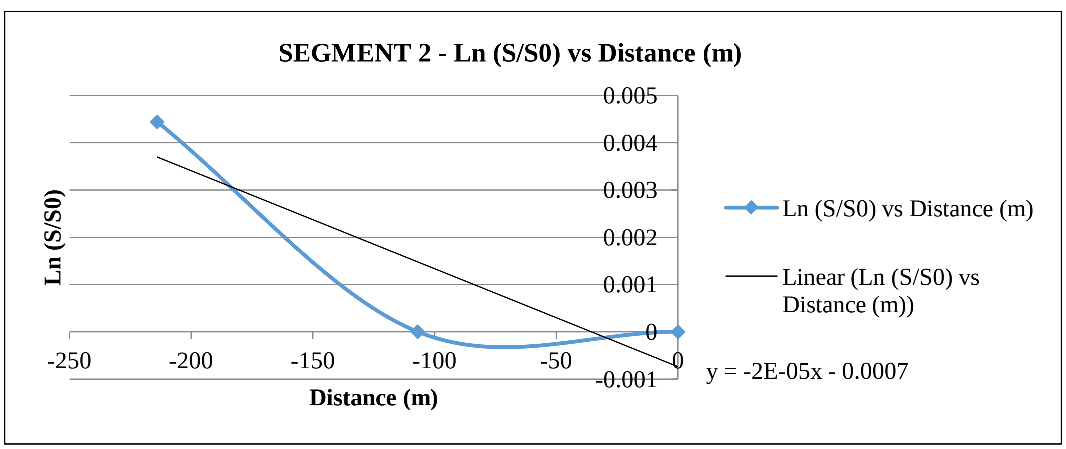

Location	Distance (m)	Salinity (ppt)	ln (S/So)	U (m/s)
1b/2a	-224	8.99	-0.005546326	
1	-112	8.91	-0.014484933	0.19
1a	0	9.04	0	
			Average U	**0.19**

E = 9500 m^2/s

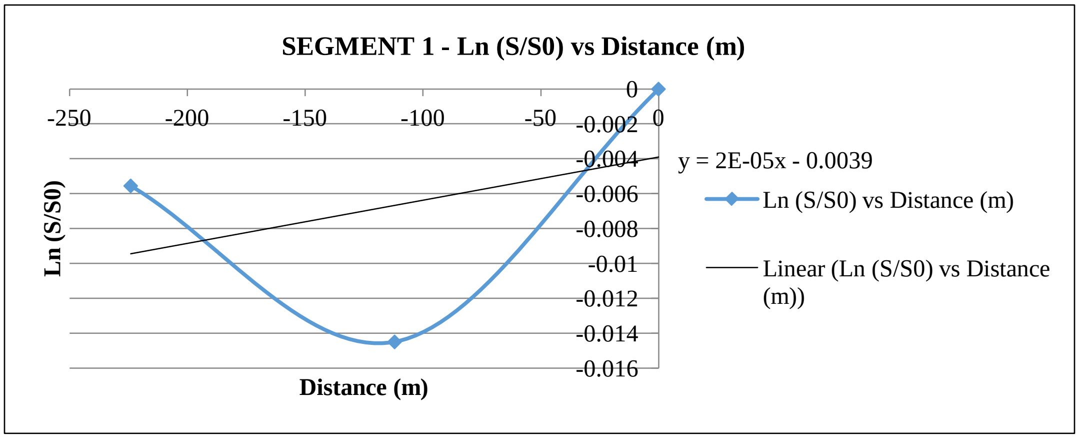

Location	Distance (m)	Salinity (ppt)	ln (S/So)	U (m/s)
8	-436.5	8.99	-0.002222223	0.18
7	-217	8.97	-0.004449396	0.27
6	0	9.01	0	0.23
			Average U	**0.23**

E = 46000 m^2/s

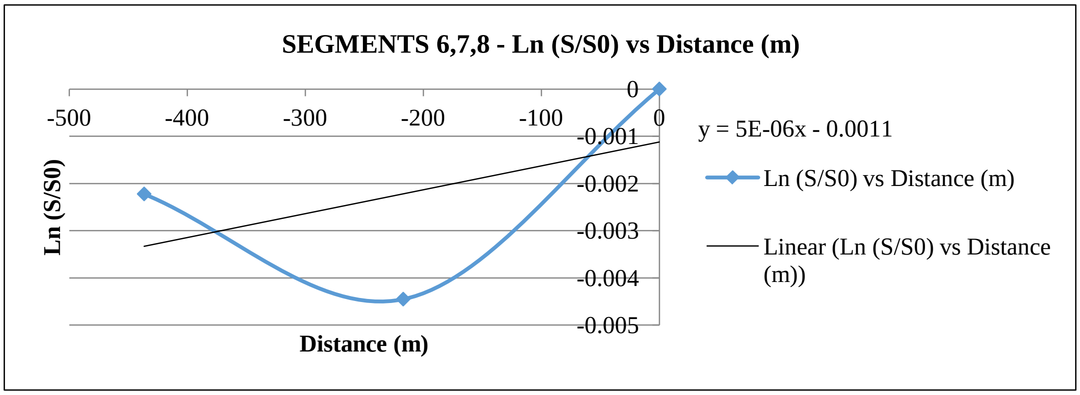

A1.3. Averaged Cycles

Location	**Distance (m)**	**Salinity (ppt)**	**U (m/s)**
5b	-1108	8.22	
5	-992.5	8.26	0.24
4b/5a	-877	8.28	
4	-767.5	8.29	0.22
3b/4a	-658	8.31	
3	-548	8.38	0.18
2b/3a	-438	8.44	
2	-331	8.46	0.23
1b/2a	-224	8.45	
1	-112	8.43	0.18
1a	0	8.53	

Location	**Distance (m)**	**Salinity (ppt)**	**U (m/s)**
8	-436.5	8.33	0.18
7	-217	8.43	0.37
6	0	8.53	0.26

Location	Distance (m)	Salinity (ppt)	ln (S/So)	U (m/s)
5b	-231	8.22	-0.007272759	
5	-115.5	8.26	-0.002418381	0.24
5a/4b	0	8.28	0	
			Average U	**0.24**

E = 8000 m^2/s

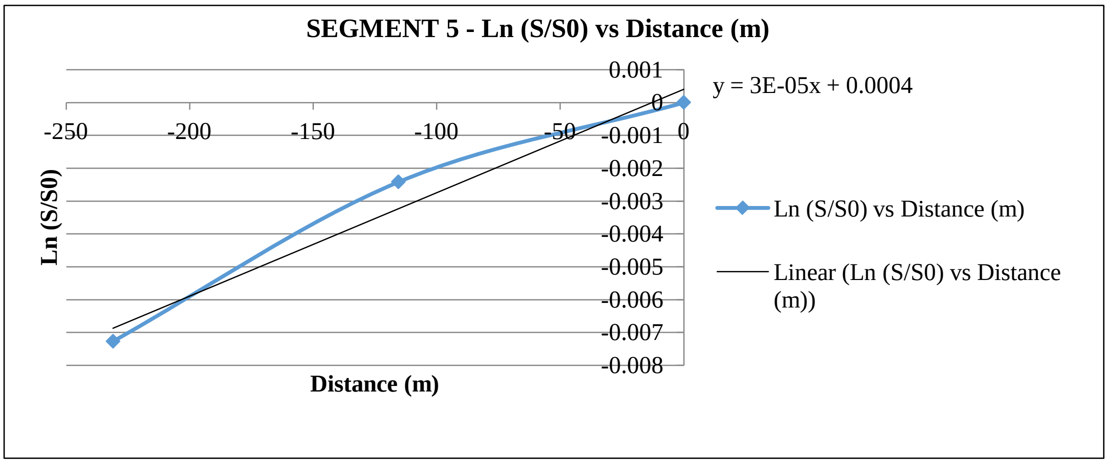

Location	Distance (m)	Salinity (ppt)	ln (S/So)	U (m/s)
4b/5a	-219	8.28	-0.00361664	
4	-109.5	8.29	-0.00240964	0.22
4a/3b	0	8.31	0	
			Average U	**0.22**

E = 11000 m^2/s

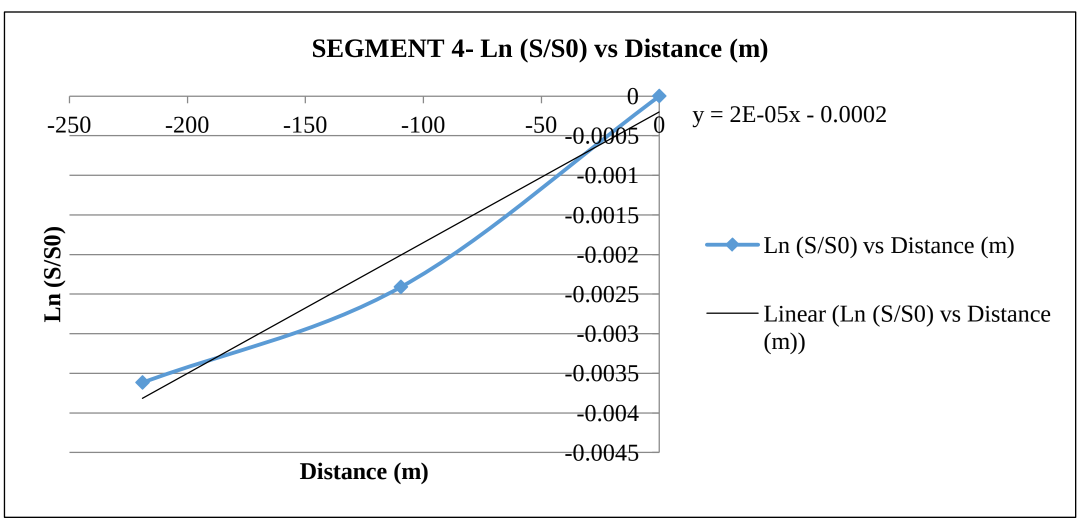

Location	Distance (m)	Salinity (ppt)	ln (S/So)	U (m/s)
3b/4a	-220	8.31	-0.0155227	
3	-110	8.38	-0.007134394	0.18
3a/2b	0	8.44	0	
			Average U	**0.18**

E = 2572 m^2/s

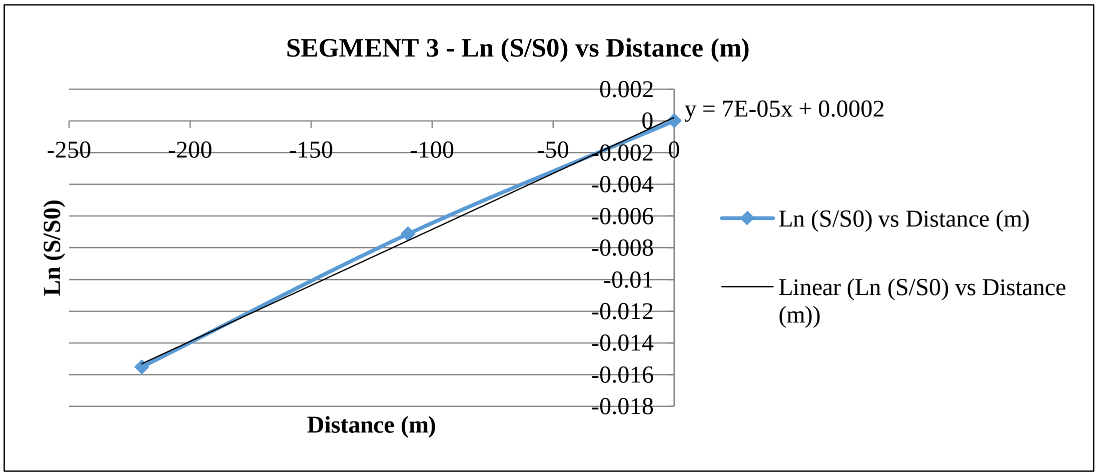

Location	Distance (m)	Salinity (ppt)	ln (S/So)	U (m/s)
2b/3a	-214	8.44	-0.001184133	
2	-107	8.46	0.001182732	0.23
2a/1b	0	8.45	0	
			Average U	**0.23**

E = 38333 m^2/s

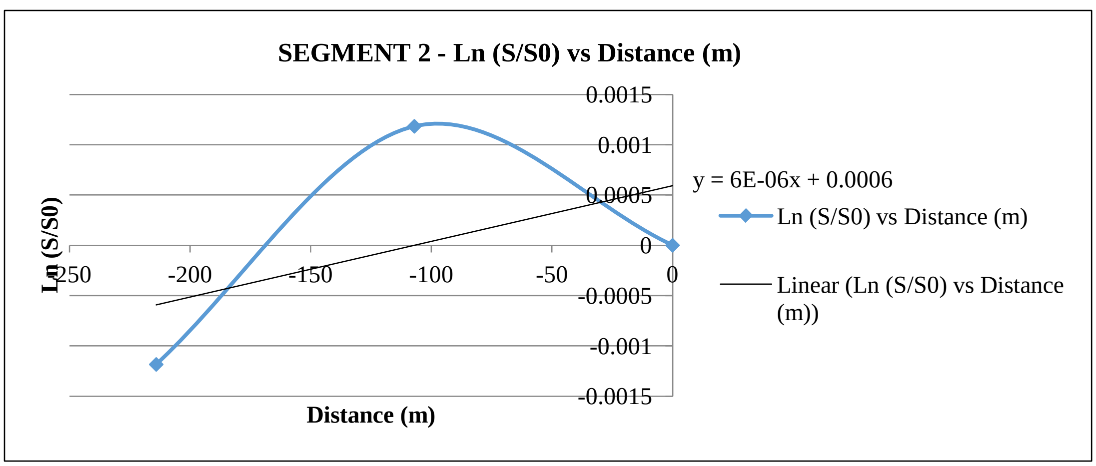

Location	Distance (m)	Salinity (ppt)	ln (S/So)	U (m/s)
1b/2a	-224	8.45	-0.00942292	
1	-112	8.43	-0.011792589	0.18
1a	0	8.53	0	
			Average U	**0.18**

E = 4500 m^2/s

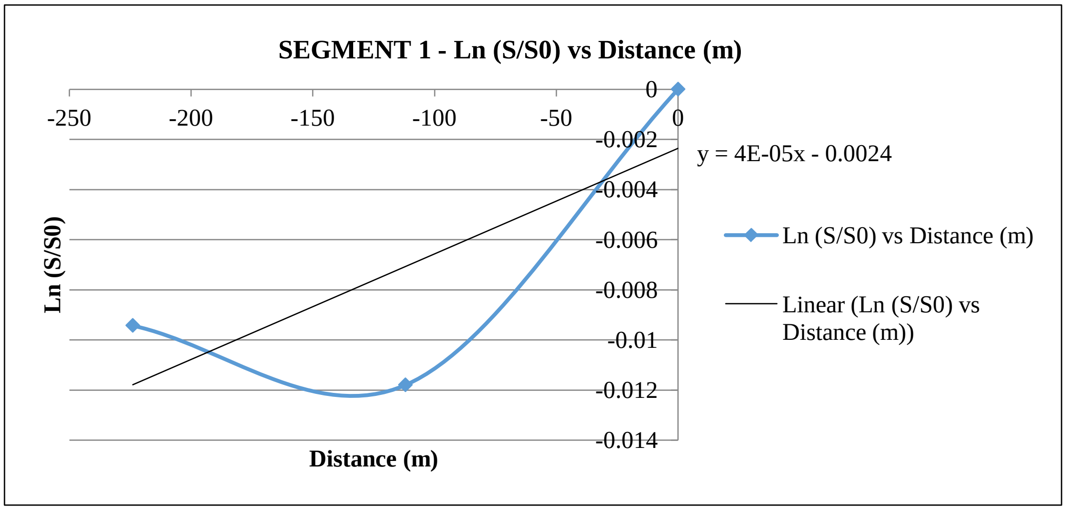

Location	Distance (m)	Salinity (ppt)	ln (S/So)	U (m/s)
8	-436.5	8.33	-0.023725905	0.18
7	-217	8.43	-0.011792589	0.37
6	0	8.53	0	0.26
			Average U	**0.27**

E = 5400 m^2/s

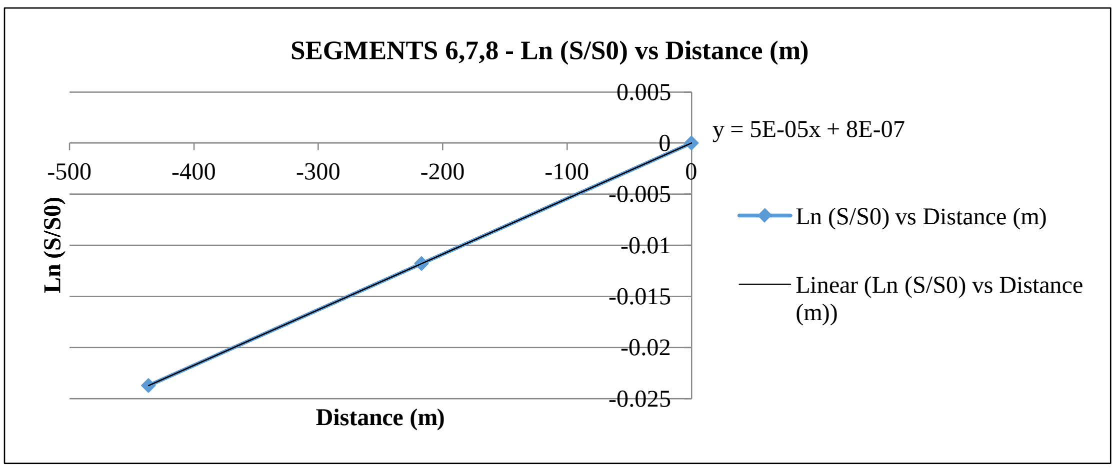

APPENDIX II.
TIDAL CYCLE FLOW AND NET ESTUARINE FLOW

A2.1. Tidal Cycle Flow – Ebb Cycle

Segment	Distance* (m)	Interface	Cross sectional Area (X direction) (m^2)	U (m/s)	Q (m^3/s)
5	-880.5		83.38	0.3	25.01
		5,4	85.67	0.285	24.42
4	-655.5		87.95	0.27	23.75
		4,3	87.75	0.225	19.74
3	-436		87.54	0.18	15.76
		3,2	88.77	0.225	19.97
2	-219		90	0.27	24.3
		2,1	87.99	0.225	19.8
1	0		85.98	0.18	15.48

* from centroide

Segment	Distance* (m)	Interface	Cross sectional Area (X direction) (m^2)	U (m/s)	Q (m^3/s)
5'	-880.5		83.38	0.19	15.84
		5',8	85.67	0.19	16.28
8	-655.5		87.95	0.19	16.71
		8,7	87.75	0.335	29.4
7	-436		87.54	0.48	42.02
		7,6	88.77	0.385	34.18
6	-219		90	0.29	26.1
		6,1'	87.99	0.29	25.52
1'	0		85.98	0.29	24.93

* from centroide

Segment	Distance* (m)	Interface	Cross sectional Area (Y direction) (m^2)	U (m/s)	Qy (m^3/s)
8	-147.5		197.1	0.19	37.45
		8,4	147.83	0.23	34
4	0		98.55	0.27	26.61

* from centroide

Segment	Distance* (m)	Interface	Cross sectional Area (Y direction) (m^2)	U (m/s)	Qy (m^3/s)
7	-145.5		198	0.48	95.04
		7,3	148.5	0.33	49.01
3	0		99	0.18	17.82

* from centroide

Segment	Distance* (m)	Interface	Cross sectional Area (Y direction) (m^2)	U (m/s)	Qy (m^3/s)
6	-148.6		192.6	0.29	55.85
		6,2	144.45	0.28	40.45
2	0		96.3	0.27	26

* from centroide

A2.2. Tidal Cycle Flow – Flood Cycle

Segment	Distance* (m)	Interface	Cross sectional Area (X direction) (m^2)	U (m/s)	Q (m^3/s)
5	-880.5		83.38	0.18	15.01
		5,4	85.67	0.175	14.99
4	-655.5		87.95	0.17	14.95
		4,3	87.75	0.17	14.92
3	-436		87.54	0.17	14.88
		3,2	88.77	0.18	15.98
2	-219		90	0.19	17.1
		2,1	87.99	0.19	16.72
1	0		85.98	0.19	16.34

* from centroide

Segment	Distance* (m)	Interface	Cross sectional Area (X direction) (m^2)	U (m/s)	Q (m^3/s)
5'	-880.5		83.38	0.18	15.01
		5',8	85.67	0.18	15.42
8	-655.5		87.95	0.18	15.83
		8,7	87.75	0.225	19.74
7	-436		87.54	0.27	23.64
		7,6	88.77	0.25	22.19
6	-219		90	0.23	20.7
		6,1'	87.99	0.23	20.24
1'	0		85.98	0.23	19.78

* from centroide

Segment	Distance* (m)	Interface	Cross sectional Area (Y direction) (m^2)	U (m/s)	Qy (m^3/s)
8	-147.5		197.1	0.18	35.48
		8,4	147.83	0.175	25.87
4	0		98.55	0.17	16.75

* from centroide

Segment	Distance* (m)	Interface	Cross sectional Area (Y direction) (m^2)	U (m/s)	Qy (m^3/s)
7	-145.5		198	0.27	53.46
		7,3	148.5	0.22	32.67
3	0		99	0.17	16.83

* from centroide

Segment	Distance* (m)	Interface	Cross sectional Area (Y direction) (m^2)	U (m/s)	Qy (m^3/s)
6	-148.6		192.6	0.23	44.3
		6,2	144.45	0.21	30.33
2	0		96.3	0.19	18.3

* from centroide

A2.3. Net Estuarine Flow

Segment	Distance* (m)	Interface	Cross Sec. Area (X direction) (m^2)	U Ebb (m/s)	Q Ebb (m^3/s)	U Flood (m/s)	Q Flood (m^3/s)	Qn (m^3/s)
5	-880.5		83.38	0.3	25.01	0.18	15.01	4.16
		5,4	85.67	0.285	24.42	0.175	14.99	3.97
4	-655.5		87.95	0.27	23.75	0.17	14.95	3.75
		4,3	87.75	0.225	19.74	0.17	14.92	2.38
3	-436		87.54	0.18	15.76	0.17	14.88	1.03
		3,2	88.77	0.225	19.97	0.18	15.98	2.15
2	-219		90	0.27	24.3	0.19	17.1	3.31
		2,1	87.99	0.225	19.8	0.19	16.72	1.87
1	0		85.98	0.18	15.48	0.19	16.34	0.51

* from centroide

Segment	Distance* (m)	Interface	Cross Sec. Area (X direction) (m^2)	U Ebb (m/s)	Q Ebb (m^3/s)	U Flood (m/s)	Q Flood (m^3/s)	Qn (m^3/s)
5'	-880.5		83.38	0.19	15.84	0.18	15.01	1.02
		5',8	85.67	0.19	16.28	0.18	15.42	1.05
8	-655.5		87.95	0.19	16.71	0.18	15.83	1.08
		8,7	87.75	0.34	29.84	0.23	20.18	4.3
7	-436		87.54	0.48	42.02	0.27	23.64	7.46
		7,6	88.77	0.39	34.62	0.25	22.19	5.35
6	-219		90	0.29	26.1	0.23	20.7	2.86
		6,1'	87.99	0.29	25.52	0.23	20.24	2.8
1'	0		85.98	0.29	24.93	0.23	19.78	2.73

* from centroide

Segment	Distance* (m)	Interface	Cross Sec. Area (Y direction) (m^2)	U Ebb (m/s)	Q Ebb (m^3/s)	U Flood (m/s)	Q Flood (m^3/s)	Qn (m^3/s)
8	-147.5		197.1	0.19	37.45	0.18	35.48	2.41
		8,4	147.83	0.23	34	0.175	25.87	4.05
4	0		98.55	0.27	26.61	0.17	16.75	4.2

* from centroide

Segment	Distance* (m)	Interface	Cross Sec. Area (Y direction) (m^2)	U Ebb (m/s)	Q Ebb (m^3/s)	U Flood (m/s)	Q Flood (m^3/s)	Qn (m^3/s)
7	-145.5		198	0.48	95.04	0.27	53.46	16.87
		7,3	148.5	0.33	49.01	0.22	32.67	7.2
3	0		99	0.18	17.82	0.17	16.83	1.16

* from centroide

Segment	Distance* (m)	Interface	Cross Sec. Area (Y direction) (m^2)	U Ebb (m/s)	Q Ebb (m^3/s)	U Flood (m/s)	Q Flood (m^3/s)	Qn (m^3/s)
6	-148.6		192.6	0.26	50.08	0.23	44.3	4.15
		6,2	144.45	0.245	35.39	0.21	30.33	3.22
2	0		96.3	0.23	22.15	0.19	18.3	2.22

* from centroide

APPENDIX III.
DISPERSION AND BULK DISPERSION COEFFICIENT CALCULATIONS PER INTERFACES

A3.1. Per Tidal Cycle – Ebb Cycle

Segment	Volume (m^3)	Distance* (m)	Interface	ΔX (m)	Cross sec. Area (X direction) (m^2)	E (m^2/s)	E'(m^3/s)
5	19260	-880.5		231		6000	
			5,4	225	85.67	6385	2431.12
4	19260	-655.5		219		6750	
			4,3	219.5	87.75	4879.27	1950.6
3	19260	-436		220		3000	
			3,2	217	88.77	4216.59	1724.92
2	19260	-219		214		5400	
			2,1	219	87.99	4227.4	1698.49
1	19260	0		224		3000	

* from centroide

Segment	Volume (m^3)	Distance* (m)	Interface	ΔX (m)	Cross sec. Area (X direction) (m^2)	E (m^2/s)	E'(m^3/s)
8	19260	-436.5		219		3200	
			8,7	219.5	87.75	3200	1279.27
7	19260	-217		220		3200	
			7,6	217	88.77	3200	1309.05
6	19260	0		214		3200	

* from centroide

Segment	Volume (m^3)	Distance* (m)	Interface	ΔY (m)	Cross sec. Area (Y direction) (m^2)	E (m^2/s)	E'(m^3/s)
8	19260	-147.5		97.5		3200	
			8,4	147.5	147.83	4383.33	4393.14
4	19260	0		195		6750	

* from centroide

Segment	Volume (m^3)	Distance* (m)	Interface	ΔY (m)	Cross sec. Area (Y direction) (m^2)	E (m^2/s)	E'(m^3/s)
7	19260	-145.5		97		3200	
			7,3	145.5	148.5	3133.33	3197.93
3	19260	0		194		3000	

* from centroide

Segment	Volume (m^3)	Distance* (m)	Interface	ΔY (m)	Cross sec. Area (Y direction) (m^2)	E (m^2/s)	E'(m^3/s)
6	19260	-148.6		100		3200	
			6,2	148.6	144.45	3933.33	3823.48
2	19260	0		200		5400	

* from centroide

A3.2. Per Tidal Cycle – Flood Cycle

Segment	Volume (m^3)	Distance* (m)	Interface	ΔX (m)	Cross sec. Area (X direction) (m^2)	E (m^2/s)	E'(m^3/s)
5	19260	-880.5		231		9000	
			5,4	225	85.67	21833.33	8313.16
4	19260	-655.5		219		34000	
			4,3	219.5	87.75	18250.46	7296.03
3	19260	-436		220		2429	
			3,2	217	88.77	6013.38	2459.94
2	19260	-219		214		9500	
			2,1	219	87.99	9500	3816.92
1	19260	0		224		9500	

* from centroide

Segment	Volume (m^3)	Distance* (m)	Interface	ΔX (m)	Cross sec. Area (X direction) (m^2)	E (m^2/s)	E'(m^3/s)
8	19260	-436.5		219		46000	
			8,7	219.5	87.75	46000	18389.52
7	19260	-217		220		46000	
			7,6	217	88.77	46000	18817.6
6	19260	0		214		46000	

* from centroide

Segment	Volume (m^3)	Distance* (m)	Interface	ΔY (m)	Cross sec. Area (Y direction) (m^2)	E (m^2/s)	E'(m^3/s)
8	19260	-147.5		97.5		46000	
			8,4	147.5	147.83	42000	42093.97
4	19260	0		195		34000	

* from centroide

Segment	Volume (m^3)	Distance* (m)	Interface	ΔY (m)	Cross sec. Area (Y direction) (m^2)	E (m^2/s)	E'(m^3/s)
7	19260	-145.5		97		46000	
			7,3	145.5	148.5	31476.33	32125.33
3	19260	0		194		2429	

* from centroide

Segment	Volume (m^3)	Distance* (m)	Interface	ΔY (m)	Cross sec. Area (Y direction) (m^2)	E (m^2/s)	E'(m^3/s)
6	19260	-148.6		100		46000	
			6,2	148.6	144.45	33833.33	32888.46
2	19260	0		200		9500	

* from centroide

A3.3. Averaged Cycles

Segment	Volume (m^3)	Distance* (m)	Interface	ΔX (m)	Cross Sec. Area (X direction) (m^2)	E (m^2/s)	E'(m^3/s)
5	19260	-880.5		231	83.38	8000	
			5,4	225	85.67	9540	3632.41
4	19260	-655.5		219	87.95	11000	
			4,3	219.5	87.75	6795.6	2716.69
3	19260	-436		220	87.54	2572	
			3,2	217	88.77	20699.7	8467.8
2	19260	-219		214	90	38333	
			2,1	219	87.99	21802.72	8759.91
1	19260	0		224	85.98	4500	

* from centroide

Segment	Volume (m^3)	Distance* (m)	Interface	ΔX (m)	Cross Sec. Area (X direction) (m^2)	E (m^2/s)	E'(m^3/s)
8	19260	-655.5		219	87.95	5400	
			8,7	219.5	87.75	5400	2158.77
7	19260	-436		220	87.54	5400	
			7,6	217	88.77	5400	2209.02
6	19260	-219		214	90	5400	

* from centroide

Segment	Volume (m^3)	Distance* (m)	Interface	ΔY (m)	Cross Sec. Area (Y direction) (m^2)	E (m^2/s)	E'(m^3/s)
8	19260	-147.5		97.5	197.1	5400	
			8,4	147.5	147.83	7266.67	7282.93
4	19260	0		195	98.55	11000	

* from centroide

Segment	Volume (m^3)	Distance* (m)	Interface	ΔY (m)	Cross Sec. Area (Y direction) (m^2)	E (m^2/s)	E'(m^3/s)
7	19260	-145.5		97	198	5400	
			7,3	145.5	148.5	4457.33	4549.23
3	19260	0		194	99	2572	

* from centroide

Segment	Volume (m^3)	Distance* (m)	Interface	ΔY (m)	Cross Sec. Area (Y direction) (m^2)	E (m^2/s)	E'(m^3/s)
6	19260	-148.6		100	192.6	5400	
			6,2	148.6	144.45	16377.67	15920.29
2	19260	0		200	96.3	38333	

* from centroide

APPENDIX IV. SAS OUTPUTS

A4.1. Univariate procedure – Identification of Statistical parameters for initial data set (3917 samples)

JAMES RIVER PLANT

EFFLUENT TSS

**** NORMALITY TEST ****

The UNIVARIATE Procedure Variable: TSS

Moments			
N	3917	**Sum Weights**	3917
Mean	8.8058207	**Sum**	34492.4
Std Deviation	8.7019972	**Variance**	75.7247567
Skewness	7.1437485	**Kurtosis**	86.0631198
Uncorrected	600272.0	**Corrected SS**	296538.147
Coeff	98.820967	**Std Error Mean**	0.13904077

Basic Statistical Measures			
Location		Variability	
Mean	8.805821	**Std Deviation**	8.7020
Median	7.000000	**Variance**	75.7247
Mode	7.000000	**Range**	172.0000
		Interquartile	5.7000

Tests for Location: Mu0=0				
Test	**Statistic**		**p Value**	
Student's t	**t**	63.33265	**Pr > |t|**	<.0001
Sign	**M**	1958.5	**Pr >= |M|**	<.0001
Signed Rank	**S**	3836702	**Pr >= |S|**	<.0001

Tests for Normality				
Test	**Statistic**		**p Value**	
Kolmogorov-Smirnov	**D**	0.205335	**Pr > D**	<0.0100
Cramer-von Mises	**W-Sq**	61.87172	**Pr > W-Sq**	<0.0050
Anderson-Darling	**A-Sq**	347.6066	**Pr > A-Sq**	<0.0050

Quantiles (Definition 5)	
Quantile	**Estimate**
100% Max	173.0
99%	40.0
95%	19.7
90%	15.0
75% Q3	10.2
50% Median	7.0
25% Q1	4.5
10%	3.0
5%	2.5
1%	1.9
0% Min	1.0

Extreme Observations			
Lowest		**Highest**	
Value	**Obs**	**Value**	**Obs**
1.0	63	100.0	3405
1.0	51	108.0	2219
1.4	3297	128.9	2231
1.4	3285	150.0	152
1.5	3706	173.0	2593

A4.2. Univariate procedure – Normality Test for sorted data set (3832 samples)

JAMES RIVER PLANT EFFLUENT TSS

**** NORMALITY TEST ****

The UNIVARIATE Procedure Variable: TSS

Moments			
N	3832	**Sum Weights**	3832
Mean	7.89050104	**Sum Observations**	30236.4
Std Deviation	4.62602283	**Variance**	21.4000872
Skewness	1.31151615	**Kurtosis**	1.9492358
Uncorrected SS	320564.08	**Corrected SS**	81983.7342
Coeff Variation	58.627745	**Std Error Mean**	0.07473001

Basic Statistical Measures			
Location		**Variability**	
Mean	7.890501	**Std Deviation**	4.62602
Median	7.000000	**Variance**	21.40009
Mode	7.000000	**Range**	26.00000
		Interquartile Range	5.60000

Tests for Location: Mu0=0				
Test	**Statistic**		**p Value**	
Student's t	**t**	105.5868	**Pr > |t|**	<.0001
Sign	**M**	1916	**Pr >= |M|**	<.0001
Signed Rank	**S**	3672014	**Pr >= |S|**	<.0001

Tests for Normality				
Test	**Statistic**		**p Value**	
Kolmogorov-Smirnov	**D**	0.12417	**Pr > D**	<0.0100
Cramer-von Mises	**W-Sq**	14.87134	**Pr > W-Sq**	<0.0050
Anderson-Darling	**A-Sq**	93.61157	**Pr > A-Sq**	<0.0050

```
                    Histogram                                    #             Boxplot
 27.5+*                                                          4                *
     .**                                                        13                0
     .**                                                        10                0
     .*                                                          9                0
     .**                                                        13                0
     .**                                                        14                0
     .*                                                          9                0
     .****                                                      36                0
     .***                                                       27                0
     .*****                                                     38                0
     .*****                                                     39                |
     .******                                                    54                |
     .********                                                  69                |
 14.5+**********                                                87                |
     .***********                                               97                |
     .**************                                           124                |
     .*******************                                      167                |
     .*************************                                219             +-----+
     .******************************                           268             |     |
     .****************************************                 356             |     |
     .******************************************               374             *--+--*
     .******************************************               372             |     |
     .**************************************                   336             |     |
     .*******************************************              380             +-----+
     .*******************************************              386                |
     .********************************                         285                |
  1.5+******                                                    46                |
```

A4.3. Linear Least – Square Regression – No intercept

Linear Least-Square Regression Dependent Variable, Y: Total Suspended Solid (mg/l)

Independent Variable, X: Turbidity (NTU)

The REG Procedure Model: MODEL1 Dependent Variable: TSS

Number of Observations Read	3832
Number of Observations Used	3832

Note: No intercept in model. R-Square is redefined.

Analysis of Variance					
Source	DF	Sum of Squares	Mean Square	F Value	Pr > F
Model	1	299355	299355	54073.1	<.0001
Error	3831	21209	5.53612		
Uncorrected Total	3832	320564			

Root MSE	2.35290	R-Square	0.9338
Dependent Mean	7.89050	Adj R-Sq	0.9338
Coeff Var	29.81935		

Parameter Estimates					
Variable	DF	Parameter Estimate	Standard Error	t Value	Pr > |t|
Turbidity	1	1.71487	0.00737	232.54	<.0001

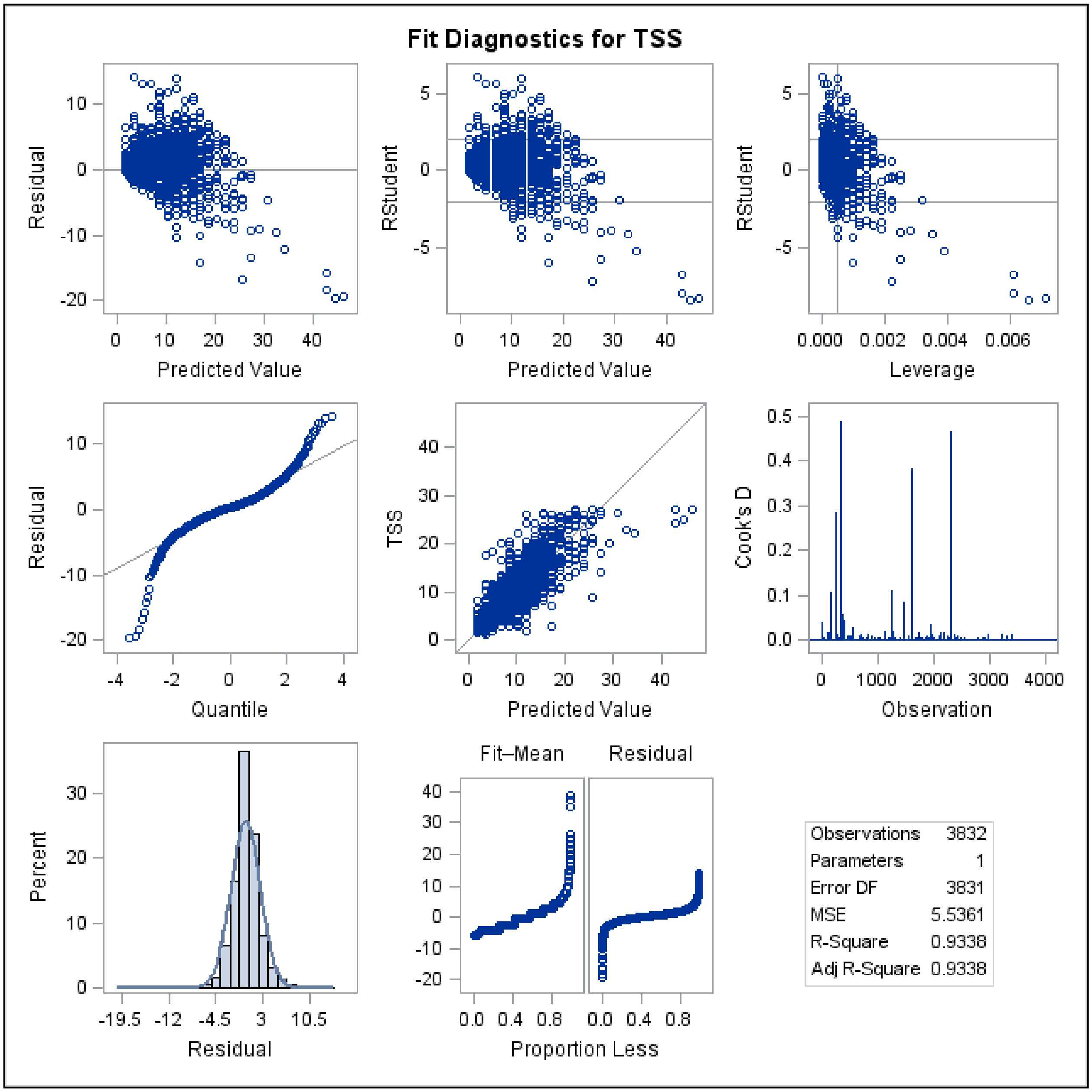

Fit Diagnostics for TSS
Residual
Predicted Value
RStudent
Predicted Value
RStudent
Leverage
Residual
Quantile
TSS
Predicted Value
Cook's D
Observation
Percent
Residual
Fit–Mean
Residual
Proportion Less
Observations 3832
Parameters 1
Error DF 3831
MSE 5.5361
R-Square 0.9338
Adj R-Square 0.9338

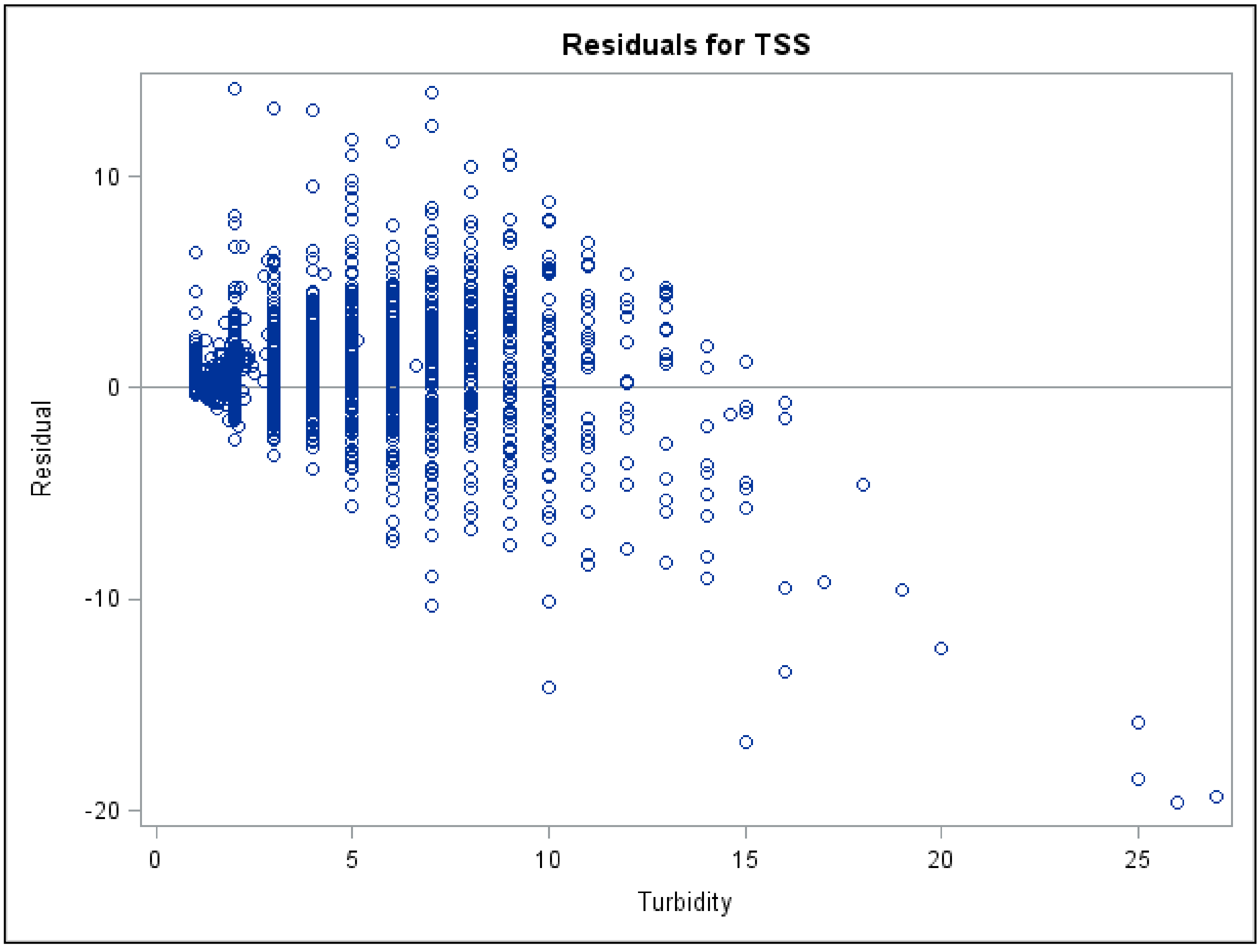
Residuals for TSS
10
0
-10
-20
Residual
0
5
10
15
20
25
Turbidity

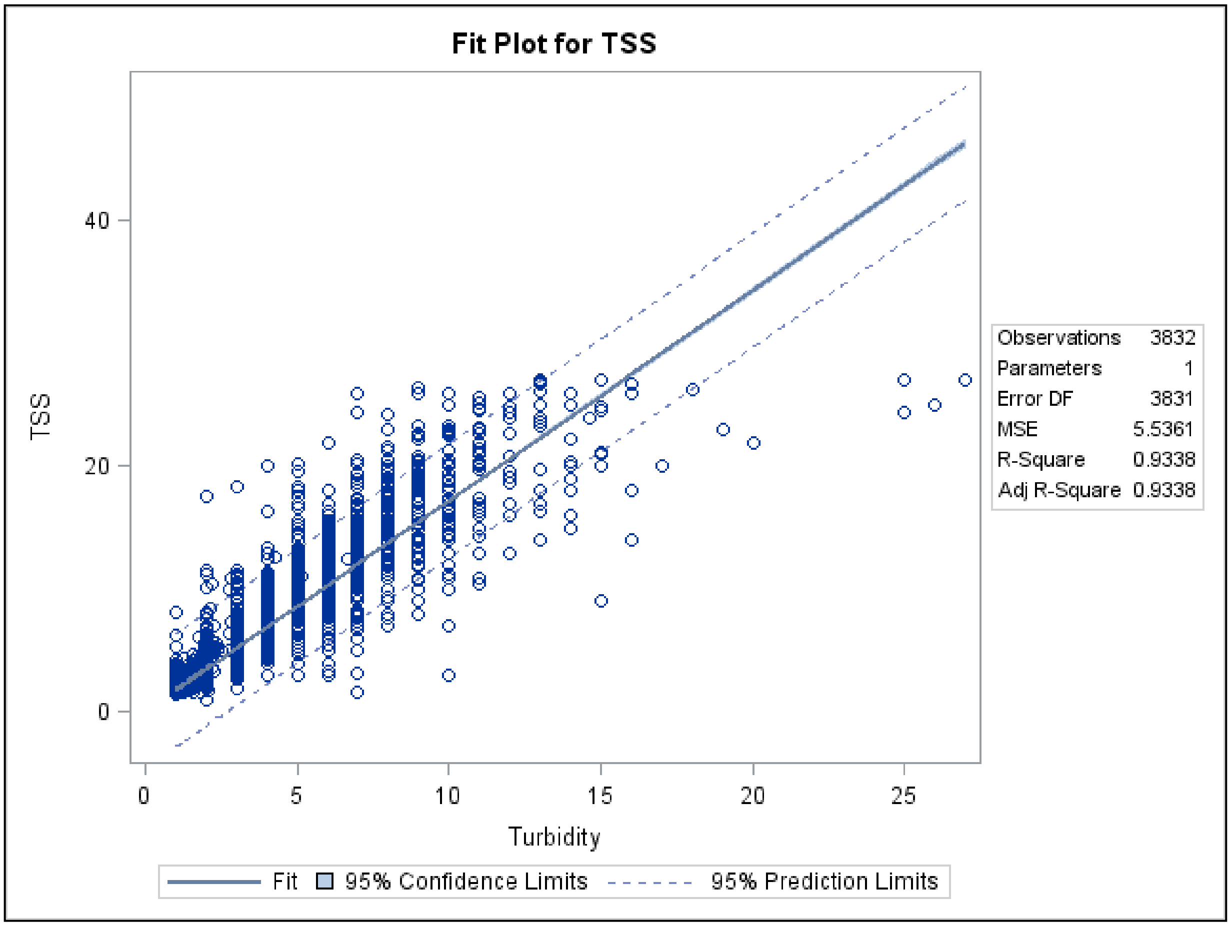
Fit Plot for TSS
TSS
Turbidity
0
20
40
0
5
10
15
20
25
Observations 3832
Parameters 1
Error DF 3831
MSE 5.5361
R-Square 0.9338
Adj R-Square 0.9338
Fit
95% Confidence Limits
95% Prediction Limits

A4.4. Multiple Means Comparison – Duncan's MRT for TSS

Multiple Means Comparison, Duncan MRT Dependent Variable, Y: Total Suspended Solid (mg/l)
Independent Variable, X: Turbidity (NTU)

The ANOVA Procedure

Class Level Information		
Class	**Levels**	**Values**
Turbidity	125	1 1.04 1.07 1.08 1.1 1.12 1.13 1.15 1.17 1.18 1.19 1.21 1.22 1.23 1.24 1.25 1.26 1.27 1.28 1.29 1.32 1.33 1.35 1.36 1.37 1.38 1.39 1.4 1.41 1.42 1.43 1.44 1.45 1.46 1.47 1.48 1.49 1.5 1.51 1.52 1.54 1.55 1.57 1.58 1.59 1.6 1.61 1.62 1.63 1.64 1.65 1.66 1.67 1.68 1.69 1.7 1.71 1.72 1.73 1.74 1.75 1.76 1.77 1.8 1.81 1.83 1.84 1.85 1.87 1.88 1.9 1.91 1.92 1.94 1.95 1.97 1.98 1.99 2 2.02 2.03 2.05 2.07 2.09 2.15 2.17 2.18 2.19 2.2 2.23
YEAR	15	2001 2002 2003 2004 2005 2006 2007 2008 2009 2010 2011 2012 2013 2014 2015

Number of Observations Read	3832
Number of Observations Used	3832

Multiple Means Comparison, Duncan MRT Dependent Variable, Y: Total Suspended Solid (mg/l)
Independent Variable, X: Turbidity (NTU)

The ANOVA Procedure

Dependent Variable: TSS

Source	DF	Sum of Squares	Mean Square	F Value	Pr > F
Model	138	81983.73424	594.08503	Infty	<.0001
Error	3693	0.00000	0.00000		
Corrected Total	3831	81983.73424			

R-Square	Coeff Var	Root MSE	TSS Mean
1.000000	0	0	7.890501

Source	DF	Anova SS	Mean Square	F Value	Pr > F
Turbidity	124	63845.14589	514.88021	Infty	<.0001
YEAR	14	30252.02679	2160.85906	Infty	<.0001

Multiple Means Comparison, Duncan MRT Dependent Variable, Y: Total Suspended Solid (mg/l) Independent Variable, X: Turbidity (NTU)

The ANOVA Procedure

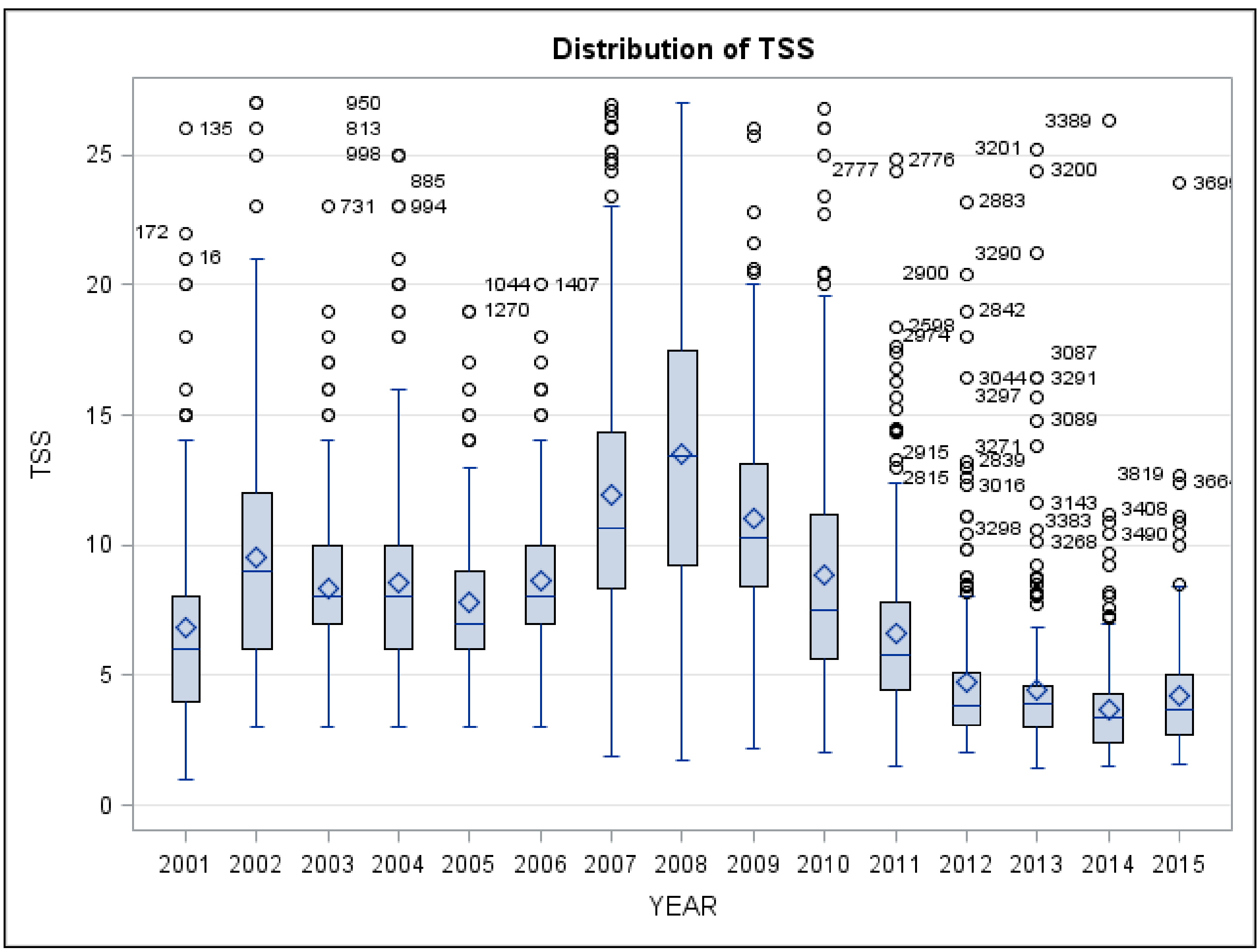

Multiple Means Comparison, Duncan MRT Dependent Variable, Y: Total Suspended Solid (mg/l)
Independent Variable, X: Turbidity (NTU)

The ANOVA Procedure Duncan's Multiple Range Test for TSS

Alpha	0.05
Error Degrees of Freedom	3693
Error Mean Square	0
Harmonic Mean of Cell Sizes	255.4232

Number of Means	**2**	**3**	**4**	**5**	**6**	**7**	**8**	**9**	**10**	**11**	**12**	**13**	**14**	**15**
Critical Range	0	0	0	0	0	0	0	0	0	0	0	0	0	0

Means with the same letter are not significantly different.			
Duncan Grouping	**Mean**	**N**	**YEAR**
A	13.48	250	2008
B	11.93	252	2007
C	11.05	260	2009
D	9.51	249	2002
E	8.84	256	2010
F	8.67	258	2006
G	8.58	253	2004
H	8.35	254	2003
I	7.82	259	2005
J	6.79	257	2001
K	6.61	255	2011
L	4.70	257	2012
M	4.44	254	2013
N	4.17	260	2015
O	3.69	258	2014

VITA

Beatriz E. Patino was born in Buga, Colombia in May 8, 1979. After finishing high school in 1996, she enrolled at Universidad del Valle in Cali Colombia and in November of 2002 obtained his undergraduate degree in Sanitary Engineering. She received a Master of Science degree in Environmental Engineering from Old Dominion University on December 2016.